ADSORPTION OF SULFUR DIOXIDE ON ACTIVATED PEANUT SHELL CHARCOAL AT VARIOUS TEMPERATURES AND ONE ATMOSPHERE PRESSURE

A THESIS

Presented to

The Faculty of the Division

of Graduate Studies

By

Arthur J. Schroeder

In Partial Fulfillment

of the Requirements for the Degree

Master of Science in Chemical Engineering

Georgia Institute of Technology

June, 1976

ADSORPTION OF SULFUR DIOXIDE ON ACTIVATED PEANUT SHELL CHARCOAL AT VARIOUS TEMPERATURES AND ONE ATMOSPHERE PRESSURE

Approved:

Michael Matteson, Chairman

Clyde Orr, Jr.

William Ernst

Date approved by Chairman: _____

ACKNOWLEDGMENTS

I wish to thank my thesis advisor, Dr. Michael J. Matteson, for his time and help in making this work possible. I would also like to thank my reading committee members, Drs. William Ernst and Clyde Orr, Jr., for their help and guidance during work on this paper and throughout my stay at Georgia Tech. A special thanks is due Dr. Albert Liabastre for countless hours of consultation and help in the lab. I also wish to thank the United States Environmental Protection Agency for financial support during this investigation. I also wish to thank my parents for their moral support and their encouragement for continuing my education.

Finally, I sincerely thank my girl friend, Miss Charlotte Young, for her help, encouragement, and tender loving care during these trying times. I promise to make it up to her.

TABLE OF CONTENTS

LIST OF TABLES

LIST OF FIGURES

SUMMARY

In this investigation the surface area, bulk and particle density, pore volume and ash content of activated carbon made from peanut hulls were characterized. This carbon was sieved to 30/45 mesh and used in a packed bed to adsorb sulfur dioxide from a nitrogen carrier stream. The effluent stream from the bed was constantly monitored for sulfur dioxide with a Beckman Infrared Analyzer. From this monitoring, breakthrough curves were generated for each test so that the outlet concentration was known as a function of time. Tests were conducted at atmospheric pressure with carrier flow rates of 100, 175, 250, 350, 500, and 700 cubic centimeters per minute and temperatures of 298, 323, 348, and 398 degrees Kelvin.

By determining the amount of sulfur dioxide adsorbed per gram of carbon from breakthrough curves, a relationship of the form

$$y[\text{gm } SO_2/\text{gm C}] = e^{aT(^\circ K)} + b$$

was seen to exist between the adsorptive capacity and the temperature of the bed.

CHAPTER I

INTRODUCTION

In recent years there has been a sharp increase in the number of coal burning power plants and other sulfur dioxide emitting sources.[4,18,35,36,38] A growing concern over the environmental impact of pollutants in the atmosphere has accompanied this rise in sulfur dioxide emissions. There are several major problems in cleaning up these emissions. The main difficulty is the large quantities of gas envolved and the relatively low concentration of the sulfur dioxide which must be removed. Three general approaches to minimizing the pollution from these sources are: (a) remove the sulfur from the original fossil fuel, (b) gasify the fuel to release the sulfur compounds before burning, and (c) burn the fuel and recover the sulfur oxides after formation. Of these, removing the sulfur dioxide after combustion is probably the most practical and most widely received.[4,9,17,38]

Wet scrubbing has found wide applications in the power industries as a method of cleaning stack gases. Wet scrubbing, however, has several inherently troublesome features. The sulfur dioxide is transferred into the water, which creates a water pollution problem; and the flue gas is usually cooled to such a level that it loses its thermal bouyancy, thus

making reheating necessary. Adsorption processes utilizing materials such as dolomite,[17,36] metal oxides,[38] and activated carbons[9,18,38,42] have been examined both in laboratories and in industrial applications. Activated carbons, which have found extensive uses in other applications[3,22] because of their high surface area and other desirable qualities, are now finding application in flue gas desulfurization.[4,9,18,36,38,42] However, there is still much unknown relative to charcoal and the fundamentals of its application in adsorption processes.

The principles of adsorption have been applied to various processes since the late eighteenth century when wood chars were used to decolorize oils, alcohols, and raw sugars.[22] These processes take advantage of the ability of certain solids to concentrate preferentially specific substances from a solution onto their surfaces. The forces which bond gas or liquid molecules to the surface of the solid are divided into two main types: physical adsorption and chemisorption. The weaker of the two, physical adsorption, is caused by the forces of molecular interaction, including permanent dipoles, induced dipoles and quadrupole action.[39] These forces, which are commonly designated as "van der Waals," cause the molecules of the adsorbate to attach themselves to the solid. Chemisorption is the result of a chemical interaction between the solid and the adsorbed substance. This chemical interaction is basically a chemical

reaction restricted to the surface layer of the adsorbent. Chemisorption generally predominates over physical adsorption in the higher temperature ranges and is characterized by large heats of adsorption.[40]

Activated carbon can be made from almost any organic substance. Some of those reviewed in the literature are coconut shells,[28,29,37] oak, maple, and pine wood,[41] peat, oxycoke,[9,18] bones, fruit pits,[22] and other sources.[11] Deitz[8] has compiled a book containing over 200 references to preparation of adsorbents from various vegetable, mineral, and animal sources. These starting materials are first ground and then charred. Frequently these products are then activated to increase the surface area and drive off impurities. Activation is usually accomplished by reheating the charred products to a high temperature while passing steam, air, water or acid over them. Varying the temperature, time, and flow rate of the process causes the pore size, surface area, and adsorption capacity of the adsorbent to increase greatly.[23,28]

Activated carbons are generally classified into two types: gas-adsorbent carbon, which adsorbs impurities from gases and recovers valuable vapors; and liquid phase or decolorizing carbon, which removes impurities from aqueous or organic liquids and solutions. Characterizing the void volume distribution which accounts for this distinction is a difficult problem since the void spaces are usually nonuniform

in shape and size. To account for these variations quantitatively, the size of the void space is frequently interpreted as a radius or diameter of a cylindrical pore and the distribution of the void volume is defined in terms of this parameter.[21,33,39] Pores are classified as macropores, transitional pores, or micropores. Macropores are conventionally specified as those having radii greater than 1000 to 2000 Å. The specific surface area of macropores are reported by M. M. Dubinin[10] to range from 0.5 to 2 m^2/g for carbonaceous adsorbents. Such values of specific surface areas indicate that macropores of active carbons do not play an appreciable role in the adsorption value. Dubinin theorizes their main function is that of a transport artery which makes the smaller internal pores of the carbon readily accessible to the molecules being adsorbed. Intermediate or transitional pores which provide the link between the macropores and the micropores are reported by Fornwalt and Hutchins[14] to lie between 50 and 500 Å in radius. It is within these transitional pores that the surface area of the adsorbent becomes an important variable, especially in liquid adsorption. The still smaller micropores, which are characteristic of most gas adsorption carbons, permit penetration by gases but are too restrictive for most liquids, especially those with long chain molecules. It is these small micropores which contribute the greatest amount of surface area to vapor adsorbent carbons.

In this work charcoal samples were first activated and then characterized according to physical properties. These samples were then utilized in a packed bed to study the effects of temperature on the ability of the charcoal to adsorb sulfur dioxide. The charcoal chosen for examintion, charred peanut shells, has been shown by Hatfield[15] to exhibit steep breakthrough curves and a high equilibrium adsorption capacity at room temperature. It is often the case that adsorption beds are used in multiple stages where one bed is on-stream while others are being regenerated.[2,6,20,40] As the maximum allowable effluent concentration is attained with one bed, it is taken off-line and replaced by a regenerated bed. The time it takes for the bed to reach the maximum allowable effluent concentration is a design parameter. Occasionally, due to changes in plant operation or economics, it may be necessary to change the temperature of a gas that passes through a column. This paper examines the effect of temperature changes on the adsorptive capacity of activated peanut shells.

CHAPTER II

EXPERIMENTAL APPARATUS AND PROCEDURE

Description of Apparatus

Breakthrough curves were obtained for various concentrations of sulfur dioxide and nitrogen flowing through a packed bed of activated carbon and then monitoring and recording the effluent concentration of sulfur dioxide as a function of time. The Matheson Gas Products SO_2 certified to be 5484 ppm sulfur dioxide with the balance nitrogen was utilized. A tank of certified pure, extra dry nitrogen from Union Carbide was used in conjunction with the Matheson gas to provide various concentrations of sulfur dioxide and to purge the system.

A schematic diagram of the apparatus is given in Figure 1. The activated carbon was packed in the inner tube of a Pyrex condensation apparatus, and 20 weight SAE Motor oil was circulated through the annulus for temperature control. The tube containing the carbon was 1 cm inside diameter, and 40 cm in length. Standard ground glass joints, which tapered down to slip inside quarter inch Tygon tubing, provided an adequate seal on the inner tube. A 15-gallon glass insulated tank provide a sufficiently large reservoir for the oil. To circulate the oil, a submerged pump, No.

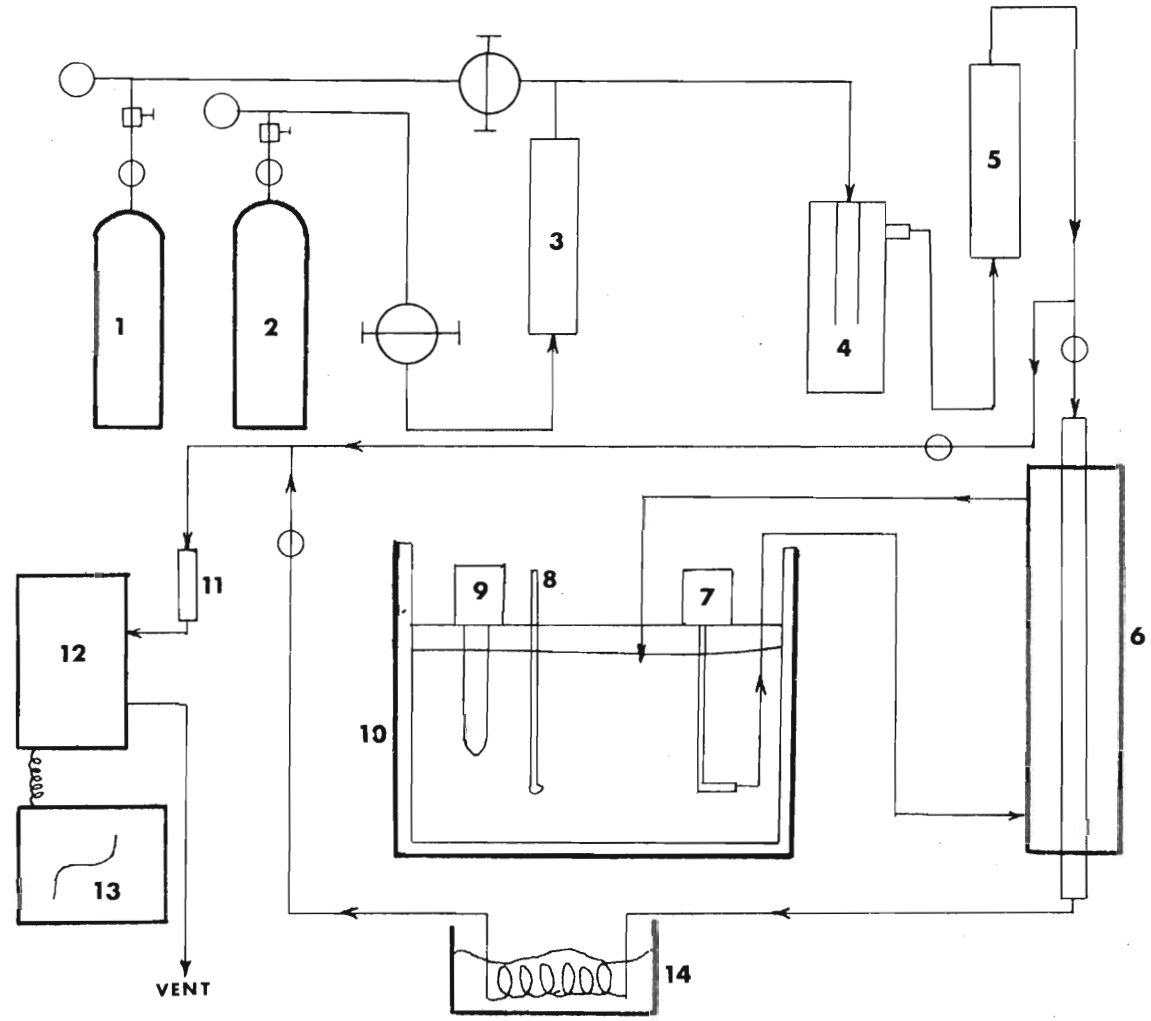

1. Extra Dry N_2

2. $SO_2 - N_2$ Mixture

3,5. Flowmeters

4. Mixing Flask

6. Packed Bed

7. Pump

8. Thermometer

9. Heater

10. Insulated Tank

11. Filter

12. SO_2 Infrared Analyzer

13. Strip Chart Recorder

14. Cooler

SYMBOLS

Cutoff Valve

Press. Reg.

Press. Gauge

Fine Metering Valve

Figure 1. Experimental Apparatus

1P295, manufactured by Dayton Electrical Manufacturing Company, was used. A 1000 watt resistance type heater-controller by Engineering Laboratory Design, Inc. controlled the temperature of the oil. A calibrated mercury thermometer, accurate to 0.5 degrees centigrade, was employed to monitor the temperature of the bath. From the thermometer it was determined that the heater-controller was able to hold the oil within a range of three degrees of the set temperature.

A Beckman 215A Infrared Analyzer, described in Appendix C-2, monitored the entrance and effluent concentrations of sulfur dioxide from the packed bed. By-pass tubing was installed around the packed bed so that periodic calibration checks could be run without comtaminating the sample. The concentration of SO_2 in nitrogen was regulated *via* two Whitey fine metering valves. Two calibrated, Matheson Model 602, rotometers (see Appendix C-1) provided accurate monitoring of the gas flow rates. To insure good mixing of the two gas streams, a glass mixing cylinder was put on line. It was necessary to cool the gas efflux from the carbon bed to within the IR operating range. The gas was passed through 5 feet of quarter inch stainless steel tubing coiled inside an ice bath. A couple of preliminary runs proved that this was a satisfactory set up over the experimental temperature range.

Experimental Procedure

A different sample of activated carbon, see Appendix A and B, was used for each experimental test. Each of these samples were degassed at 110 degrees centigrade for at least 24 hours before the test. The infrared Analyzer's calibration was checked with pure nitrogen for a zero reading on the deflection scale and with the 5484 ppm sulfur dioxide for a 100 reading. A sample of the degassed activated carbon was then weighed and placed in the packed bed. To hold the sample in place, glass wool and glass beads were packed in the bed before and after the carbon sample. The first half of the bed contained the glass beads to provide a preheat for the gas going into the carbon. It also served to disperse and spread the gas throughout the entire cross section of the bed. The last portion of the bed contained glass wool to hold the carbon in place, and keep any small particles from blowing through the system. With the carbon in place, the oil bath was brought up to the desired temperature and held there until the packed bed was able to reach thermal equilibrium with the reservoir. During this time pure nitrogen was passed through the entire system. When conditions were appropriate, the nitrogen was either turned off or mixed with the sulfur dioxide. At this time the recorder, connected with the Infrared Analyzer, was turned on to record the effluent from the packed bed. As soon as the activated carbon became completely saturated with the sulfur dioxide, the gas

and the recorder were turned off and the bed was emptied, then purged again with pure nitrogen (see Table 1).

Table 1. Sample Tests

Test #	Temperature (C°)	Flow Rate (cc/min)	Inlet Concentration (ppm SO_2)	Sample Weight (gm)	Bed Length (cm)
3a	25	150	5484	8.360	4.0
1a	25	350	5484	8.513	4.1
2a	25	700	5484	8.675	4.2
53b	25	100	5484	3.018	17.7
55b	25	175	5484	3.055	18.0
56b	25	250	5484	3.049	17.9
4b	25	350	5484	3.003	17.4
5b	25	350	2742	2.967	17.5
6b	25	350	1371	3.095	17.7
57b	25	500	5484	3.000	17.6
54b	25	700	5484	3.015	17.7
29b	50	100	5484	3.032	17.8
9b	50	175	5484	2.989	16.9
19b	50	250	5484	3.115	18.3
20b	50	350	5484	2.937	17.0
12b	50	350	2742	3.030	17.7
11b	50	350	1371	3.041	17.7

Table 1 (continued)

Test #	Temperature (C°)	Flow Rate (cc/min)	Inlet Concentration (ppm SO_2)	Sample Weight (gm)	Bed Length (cm)
10b	50	500	5484	3.053	17.8
8b	50	700	5484	3.010	17.6
17b	75	100	5484	3.100	18.1
15b	75	175	5484	3.093	18.0
31b	75	250	5484	3.027	17.8
13b	75	350	5484	3.109	18.1
21b	75	350	2742	3.164	18.5
22b	75	350	1371	3.087	18.1
18b	75	500	5484	2.957	17.0
14b	75	700	5484	3.029	17.8
28b	100	100	5484	3.024	17.8
27b	100	175	5484	3.009	17.7
30b	100	250	5484	2.976	17.5
23b	100	350	5484	3.103	18.2
24b	100	350	2742	3.009	17.7
32b	100	350	1371	3.038	17.9
26b	100	500	5484	3.024	17.8

Table 1 (continued)

Test #	Temperature (C°)	Flow Rate (cc/min)	Inlet Concentration (ppm SO_2)	Sample Weight (gm)	Bed Length (cm)
25b	100	700	5484	3.119	18.3
34b	125	100	5484	3.005	18.0
35b	125	175	5484	2.940	17.3
36b	125	250	5484	3.110	18.3
33b	125	350	5484	2.998	17.6
38b	125	350	2742	3.019	17.8
37b	125	350	1371	3.018	17.8
40b	125	500	5484	2.990	17.6
39b	125	700	5484	3.041	17.9
47c	100	350	5484	3.003	17.7
49c	75	350	5484	3.015	17.8
52c	50	350	5484	3.020	17.8
46d	100	350	5484	3.695	12.5
50e	100	500	5484		
42f	100	500	5484		
43g	100	500	5484		
44g	100	250	5484		
45g	100	125	5484		

Table 1 (concluded)

Test #	Temperature (C°)	Flow Rate (cc/min)	Inlet Concentration (ppm SO_2)	Sample Weight (gm)	Bed Length (cm)
41g	125	500	5484		
51h	100	350	5484	3.020	17.8

a) Tube diameter of 3.5 cm.; Activated charred peanut hulls used with glass wool to hold carbon in place

b) Tube diameter of 1.0 cm.; Activated charred peanut hulls used with glass wool and 15 grams of 3 mm glass beads

c) Same conditions as (b) except non-activated charred peanut hulls used

d) Same conditions as (b) except carbon from SKC Inc. lot # 105 sampling tubes used

e) Tube diameter 1.0 cm., glass wool only

f) Tube diameter 1.0 cm., glass wool and 30 gm of 3 mm glass beads

g) Tube diameter 1.0 cm., glass wool and 15 gm of 3 mm glass beads

h) Tube diameter 1.0 cm., Activated charred peanut hulls and 15 gm of 3 mm glass beads, No glass wool

CHAPTER III

EXPERIMENTAL RESULTS AND DISCUSSION

Most of the experiments were made with approximately 15 grams of 3 mm glass beads packed up stream of the carbon to provide about 25 centimeters of preheat area for the influent gases. This was found to be a satisfactory length to insure that the gas had reached bed temperature. To hold the charcoal in place, a plug of glass wool was packed in the column from the effluent side. By running several different combinations of glass beads and wool, with and without carbon in the bed, it was determined the effect on the carbon adsorption on the beads and wool was negligible. Runs 47, 49, and 52 with charred, but non-activated peanut hulls, exhibited almost no retention of the sulfur dioxide. This was expected due to the correspondingly low specific surface area. See Appendix B-1.

As described in the previous chapter, a resistance-type heater connected to a thermostatic controller was used to control the oil bath temperature. Unfortunately, the controller was only able to hold the bath temperature within about three degrees of the set temperature. After breakthrough, the effluent sulfur dioxide concentration was monitored for about two hours. During this time the chart speed on the

strip chart recorder was slowed to four inches per hour. A sinusoidal-type wave resulted as the instrument response varied from approximately 95 to 105. Due to the high non-linearity of the Beckman Infrared Analyzer in this region a small instrument response corresponded to a large concentration difference. As the temperature dropped, the carbon would adsorb more of the sulfur dioxide flowing through the bed and the recorder indicated this with a response reading around 94 to 96 which corresponds to about 4400 to 4600 ppm sulfur dioxide. It was difficult to interpret the upper portion of the breakthrough curve because of this fact. If the bath was on its cooling cycle when breakthrough occurred, the upper portion of the generated "s" shape curve would appear to approach asymptotically an instrument response of around 95, which corresponds to a reduced concentration (c/c_o) in the effluent stream of around 80. If, on the other hand, the bath was starting to heat at this time, the effluent concentration of sulfur dioxide would rise above the inlet and appear asymptotically to approach a reduced concentration of around 1.20. These two asymptotes were averaged together to yield what the curve might have looked like had the temperature been constant. These extrapolated values are indicated in Figures 2, 3, 4, 5, 6, by a dotted line extending past the solid line.

A method developed by Engel and Coull[13] to evaluate qualitatively this extrapolation of data, and to check the

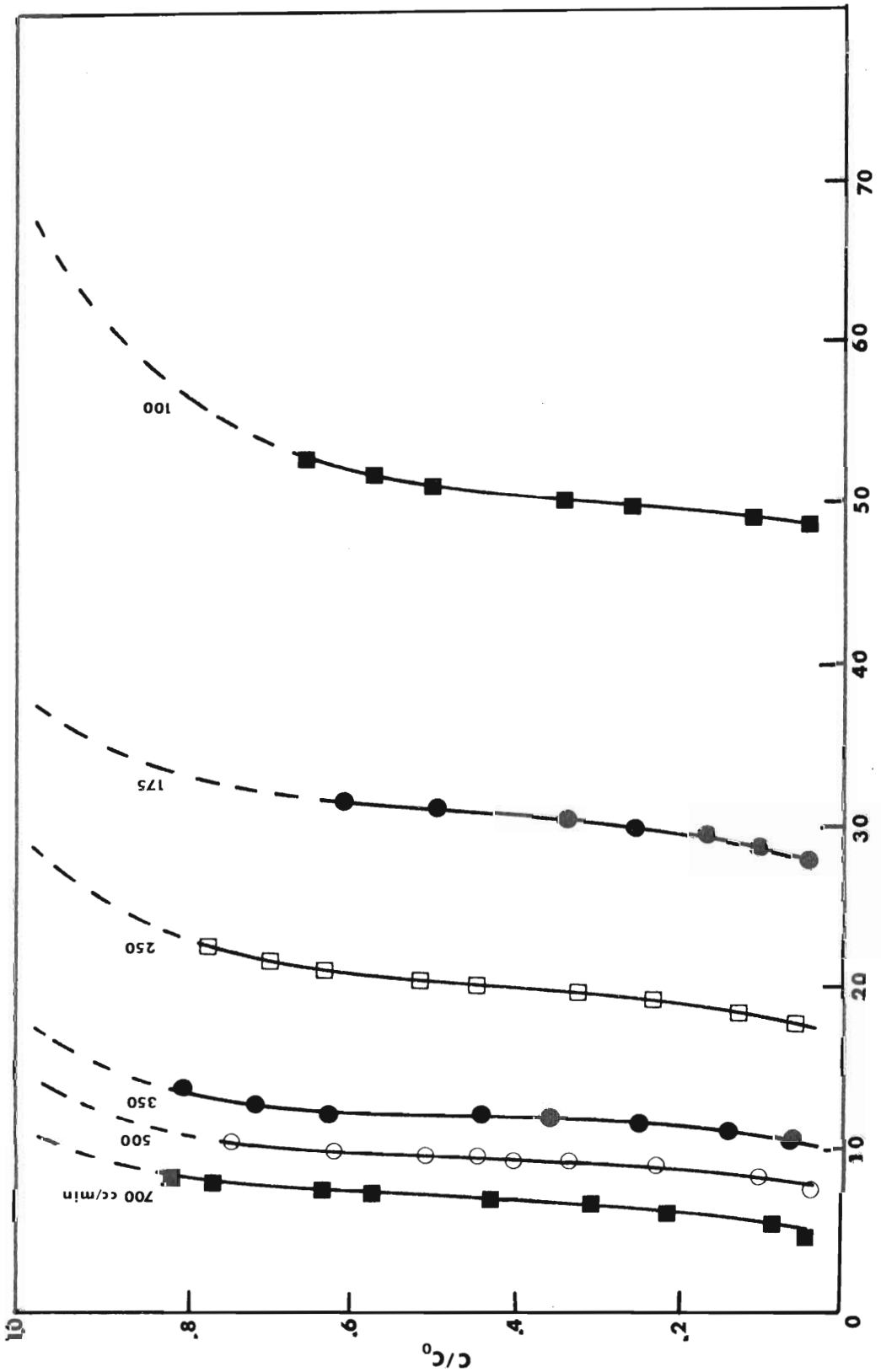

Figure 2. Breakthrough Curves for 5484 ppm SO_2 in N_2 at 25°C

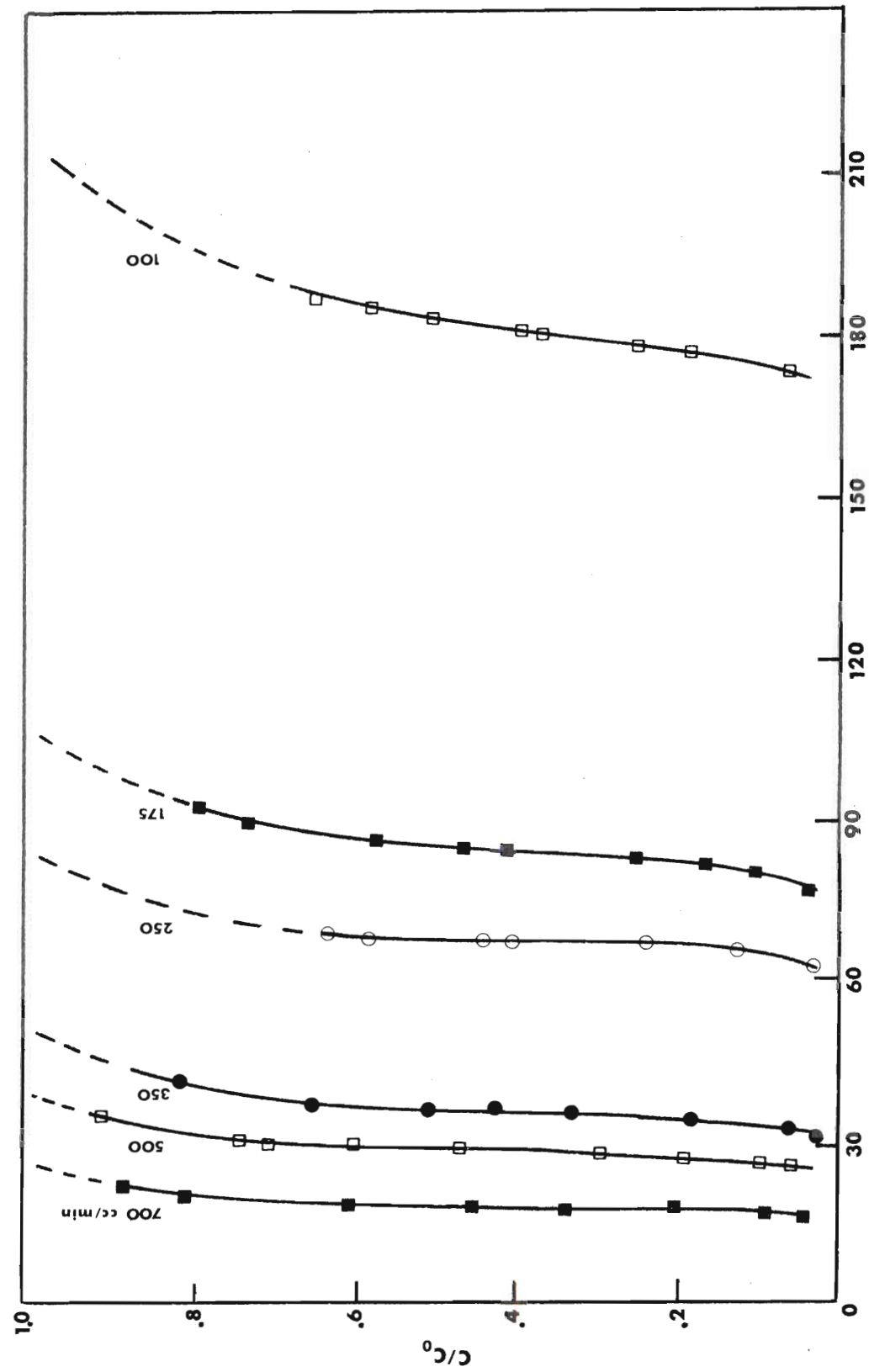

Figure 3. Breakthrough Curves for 5484 ppm SO_2 in N_2 at 50°C

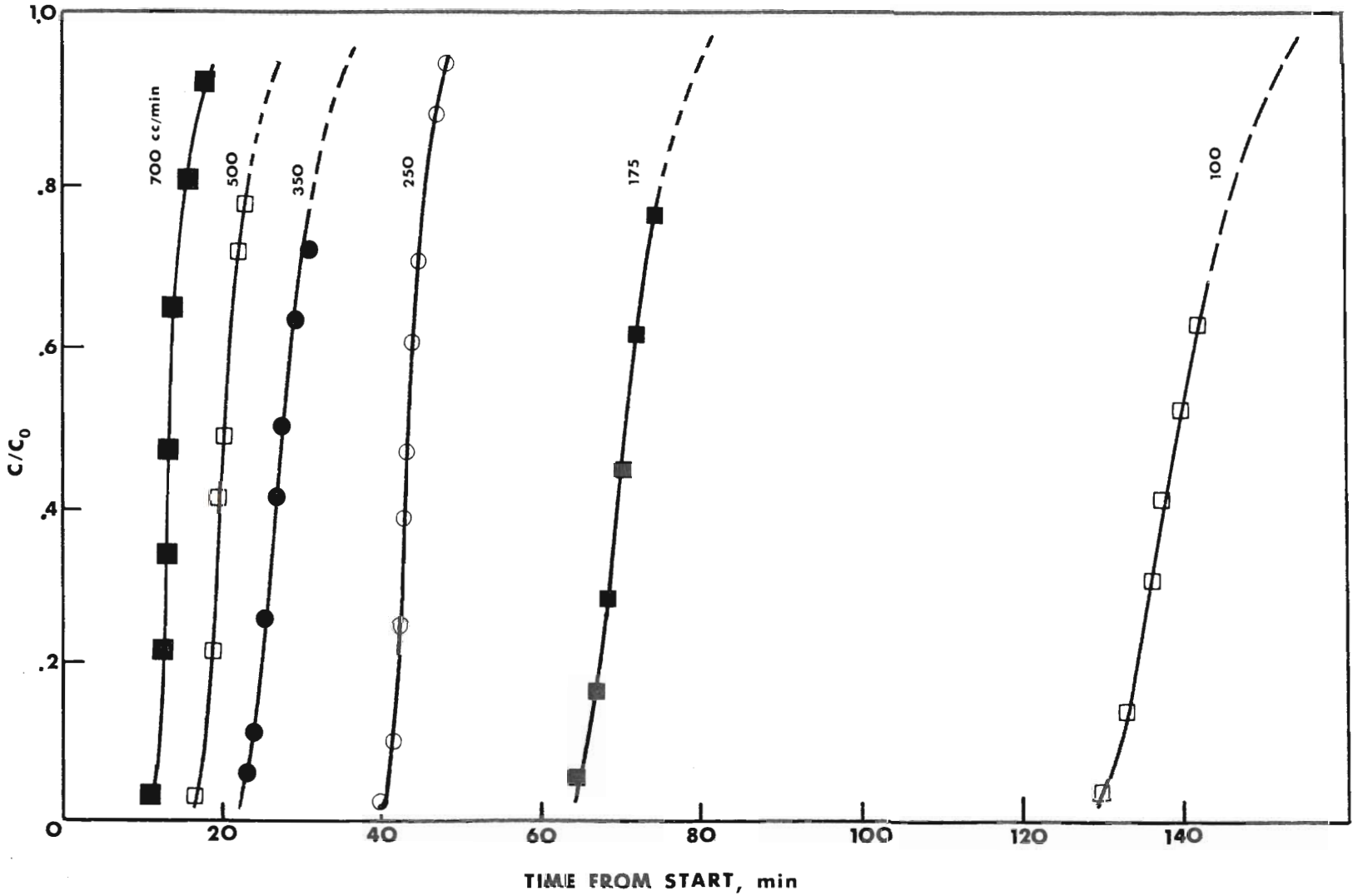

Figure 4. Breakthrough Curves for 5484 ppm SO_2 in N_2 at 75°C

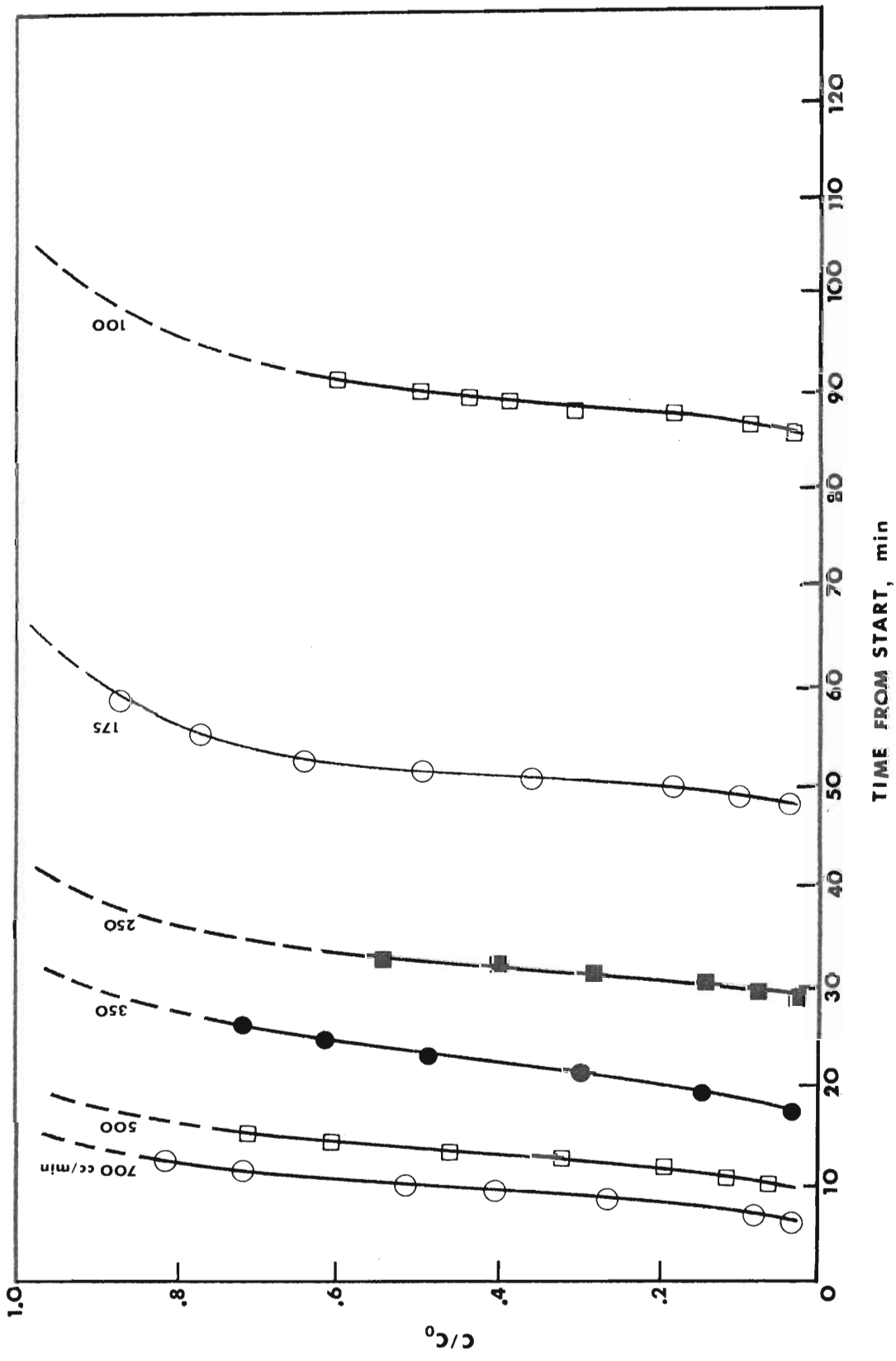

Figure 5. Breakthrough Curves for 5484 ppm SO_2 in N_2 at 100°C

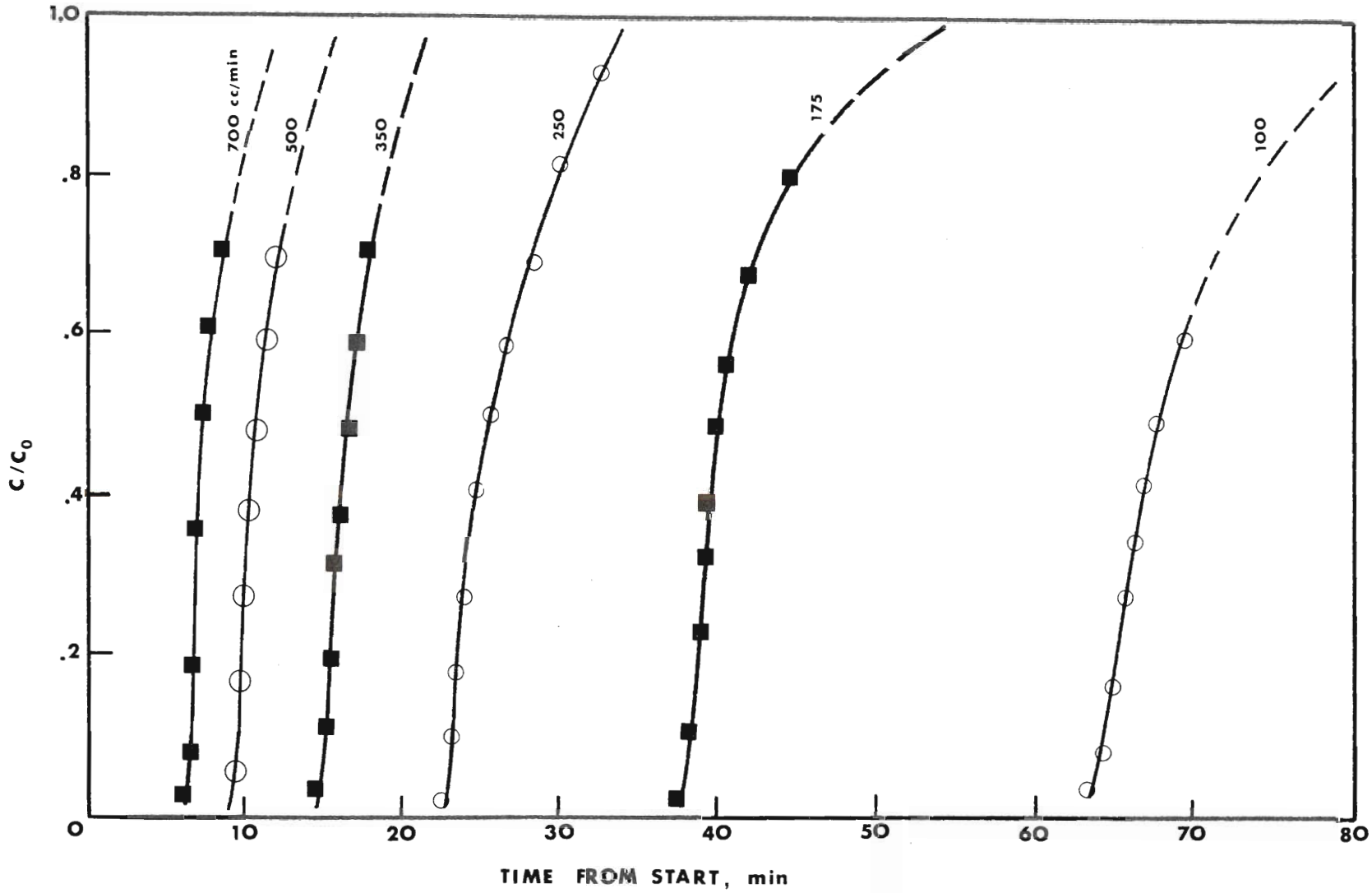

Figure 6. Breakthrough Curves for 5484 ppm SO_2 in N_2 at 125°C

lower points for consistency was employed. Kidnay[19] has reviewed this method and found that it correlates with the data very well. Basically, the method makes use of the close resemblance of the probability integral, or error curve, to the breakthrough curve. By plotting $(1 - c/c_o)100$, where c is the effluent concentration and c_o is the inlet concentration, as a function of time on normal probability paper, a fairly straight line should result. Figure 7 shows a fairly good fit of experimental data with this method.

Earlier work in this laboratory by Hatfield,[15] compared two commercially available carbons and charcoals made from waste rubber and peanut hulls with Rosen's[30,31] theoretical solutions. Hatfield's fifth run, which was the only one that could be compared with this work, was at 285 cc/min, 78°F, 5005 ppm sulfur dioxide in nitrogen at atmospheric pressure. With his 10% breakthrough ($c/c_o = 0.1$) at 107.5 min., the bed had adsorbed 0.0661 gm sulfur dioxide per gram of carbon. This falls between the values shown in Figure 8 for 250 cc/min and 350 cc/min at 298°K.

Each set of points in Figure 8 were fit by a straight line using a least squares fit. By then inserting the temperature values into the equation for each flow rate, a percent deviation from the actual amount adsorbed per gram of carbon was calculated as seen in Table 2. The overall average deviation of the calculated values using the equation

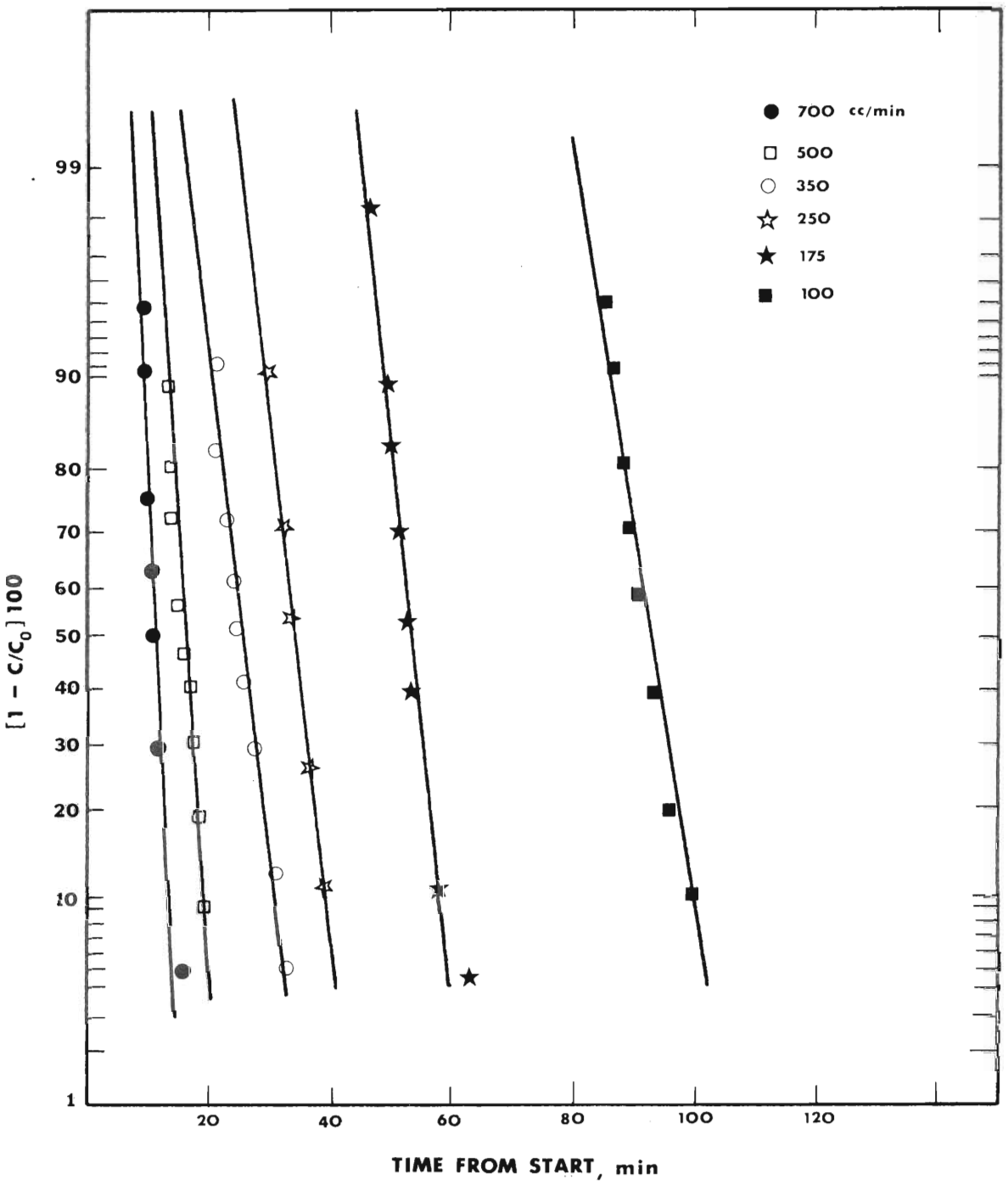

Figure 7. Correlation of Data at 75°C by Method of Engel and Coull [13]

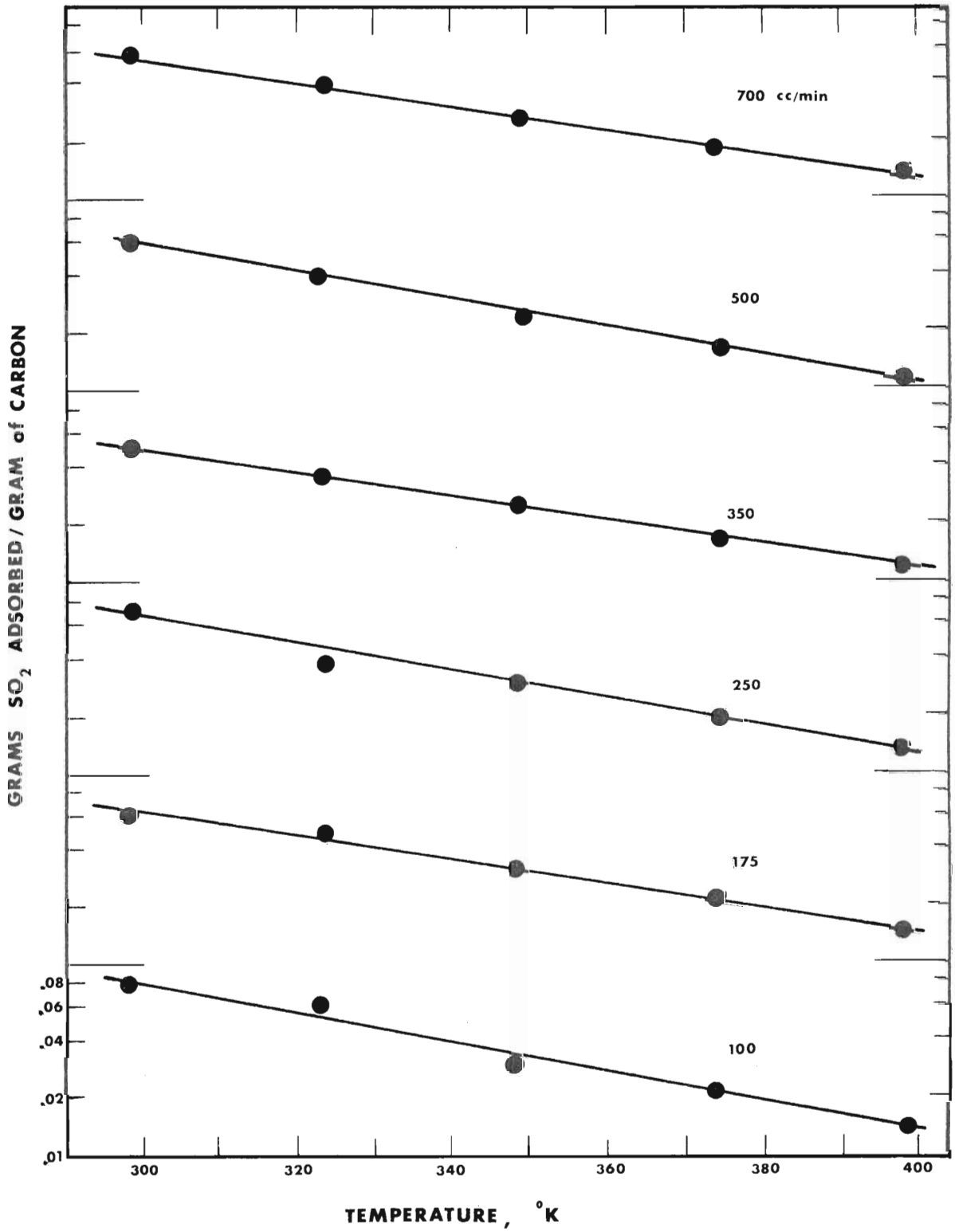

Figure 8. Adsorption Capacity per Gram of Charcoal vs Temperature, $C/C_o = 0.1$

Table 2. Temperature-Adsorption Correlations

Flow (cc/min)	Temperature (°K)	Actual gm SO_2/gm C	Calculated gm SO_2/gm C	Deviation %	Coefficients of Equation 1
100	298	0.08424	0.08852	5.1	a = -.01675
	323	0.06714	0.05824	13.3	b = 2.5667
	348	0.03456	0.03831	10.8	
	373	0.02463	0.02521	2.3	
	398	0.01714	0.01658	3.2	
175	298	0.06731	0.06912	2.7	a = -.01321
	323	0.05245	0.04968	5.3	b = 1.2647
	348	0.03459	0.03571	5.2	
	373	0.02570	0.02566	0.1	
	398	0.01844	0.01845	0.03	
250	298	0.07679	0.07036	8.3	a = -.01528
	323	0.04403	0.04802	9.0	b = 1.8990
	348	0.03139	0.03277	4.4	
	373	0.02227	0.02237	0.5	
	398	0.01599	0.01527	4.5	

Table 2 (concluded)

Flow (cc/min)	Temperature (°K)	Actual gm SO_2/gm C	Calculated gm SO_2/gm C	Deviation %	Coefficients of Equation 1
350	298	0.05257	0.05381	2.3	a = -.01360
	323	0.03869	0.03830	1.0	b = 1.1311
	348	0.02839	0.02918	2.7	
	373	0.01903	0.01940	1.9	
	398	0.01369	0.01381	0.8	
500	298	0.06775	0.06251	7.7	a = -.015538
	323	0.04254	0.04239	0.4	b = 1.8578
	348	0.02517	0.02874	14.2	
	373	0.01823	0.01949	6.9	
	398	0.01484	0.01322	10.9	
700	298	0.05603	0.05435	2.9	a = -.01350
	323	0.03883	0.03878	0.3	b = 1.1109
	348	0.02700	0.02767	2.5	
	373	0.01829	0.01974	7.9	
	398	0.01510	0.01409	6.7	

$$y[\text{gm } SO_2/\text{gm C}] = e^{aT(^\circ K) + b}$$

was 4.7 percent. Even though there was no definite relationship between the empirical values of a and b and the flowrate, there seemed to be a slight general decrease in adsorption capacity as the flow rate increased.

CHAPTER IV

CONCLUSIONS AND RECOMMENDATIONS

The carbon used in this work was made from peanut hulls, a cheap and readily available starting material. It was fully evaluated and characterized (see Appendix B). With this activated carbon it has been shown that there is an exponential relationship of the form

$$y[\text{gm } SO_2/\text{gm C}] = e^{aT(^\circ K) + b}$$

relating the adsorption capacity of the carbon with temperature under unsteady state-fixed bed conditions. This relationship was developed from breakthrough curves over a range of flowrates, 100 cubic centimeters per minute up to 700 cubic centimeters per minute.

Mahajan, et al.[25] have shown with the same type of carbon, and by changing the activation temperature, that substantial changes can be made in the adsorption capacity of the charcoal. It seems reasonable to believe that there should be a maximum surface area or adsorption capacity at some optimum activation temperature. A more detailed investigation may show that peanut hulls exhibit even greater adsorption capacity at some other activation temperature.

The relationship found between adsorption capacity and temperature for fixed beds in this paper should be examined for application with other charcoals. By comparing with other carbons, perhaps the variables 'a' and 'b' could be related in some way with the surface area of the adsorbent or the pore size.

APPENDICES

APPENDIX A

PREPARATION OF ACTIVATED CARBON

The adsorbent used in this study is a microporous activated carbon with a heterogeneous surface prepared from charred peanut shells provided from the Engineering Experiment Station at the Georgia Institute of Technology. A reactor for the process was made from a two-inch diameter standard steel water pipe which was cut to eighteen inches in length and then threaded on both ends. Threaded pipe caps were then used to close off both ends. One of the pipe caps was drilled and tapped for a one-eighth inch Swagelock fitting for gas and water injection and the other was fitted with an extension pipe which led to an exhaust vent. Heat for the process was provided by a Lindberg electrical heavy duty tube furnace. (See Figures 9 and 10.)

The first two inches of the reactor were packed with one-half inch Berl Saddles. The middle section of the tube was packed with a weighted amount of sieved 30/45 mesh charred peanut shells. The remaining two inches was packed with more Berl Saddles. A uniform heating zone was attained by placing the charred peanut shells in the middle of the reactor tube. The Berl Saddles also served to disperse the incoming gas stream. The caps were then tightened and the

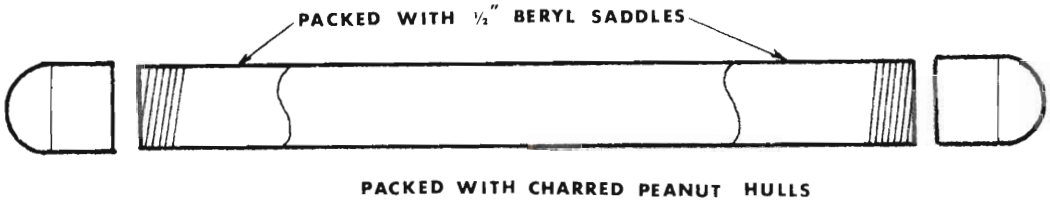

Figure 9. Reaction Tube

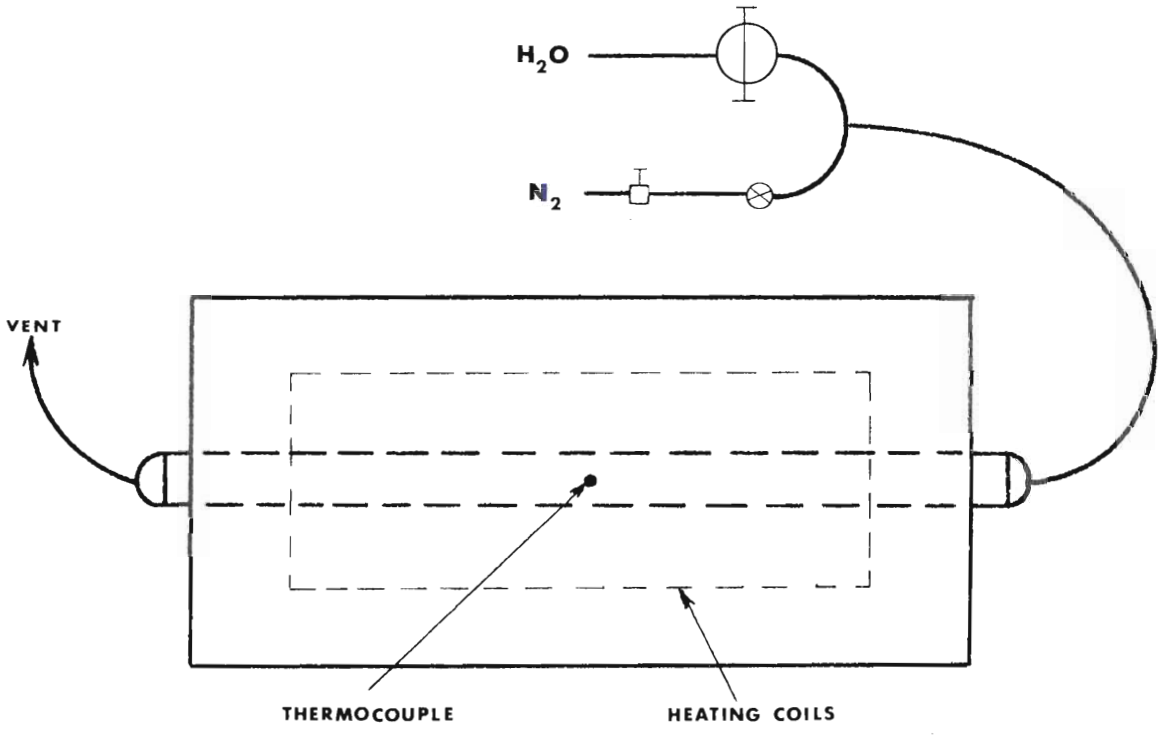

Figure 10. Oven with Reaction Tube Inserted

reactor was heated to 800°C. This temperature was maintained for thirty minutes after which water was injected through the Swagelock fitting at the rate of one gram of water per gram of carbon sample per hour for thirty mintues. After water injection the sample was kept at 800°C for thirty additional minutes before cooling was initiated. The cooling was aided by slowly passing nitrogen through the reactor to minimize oxidation of the carbon.

When the reactor was sufficiently cool, the samples were again sieved to 30/45 mesh size to insure a uniform particle size. The carbon was then stored in air-tight containers. Since the process was a batch operation, each sample was labeled and stored separately so that possible deviations between batches could be determined.

APPENDIX B

CHARACTERIZATION OF ACTIVATED CARBON

B-1. Surface Area Analysis

The surface area of the adsorbents was measured with a Micromeritics Instrument Corporation, Model 2200, High Speed Surface Area Analyzer. The determination of surface areas by this machine is based on the principles developed by Brunauer, Emmett, and Teller.[a] One form of the BET equation is

$$\frac{P/P_s}{V[1-(P/P_s)]} = \frac{1}{V_m C} + \frac{C-1}{V_m C}\frac{P}{P_s} \qquad (1)$$

where V is the volume (at standard temperature and pressure conditions) of the gas adsorbed at pressure P, P_s is the saturation pressure of the adsorbate at the isotherm temperature T, V_m is the volume of gas required to form an adsorbed monomolecular layer, and C is a constant related to the energy of adsorption. By plotting experimental values of the left hand side of equation (1) on the ordinate against P/P_s on the abscissa, it has been shown[b] that a straight line results for P/P_s values between about 0.05 and 0.35. The surface area of the adsorbent sample is calculated from the monolayer covering gas volume V_m, which is equal to the reciprocal of

the sum of the slope and the intercept of equation (1). Using nitrogen as an adsorbate and 16.2 $\mathring{A}^2$ as the area covered by one of its molecules,[c] the relationship giving the sample surface area, S, becomes

$$S = \frac{4.35}{(\text{slope} + \text{intercept})} \qquad (2)$$

The Micromeritics Analyzer does not make use of the actual intercept but makes an allowance for this induced error by holding the nitrogen gas to be adsorbed in a slightly smaller chamber than theory would require. The analyzer actually measures the volume of gas adsorbed between the ice water temperature point and the temperature of liquid nitrogen. By various parameters, the machine was thus designed to give fairly rapid and accurate values for surface areas of porous solids. The instruction manual[b] should be consulted for the details of operation.

To determine the reproducability of the analyzer's results, two different samples were each analyzed three different times to measure the standard deviation between the resulting surface areas. The first sample, used in runs one through three, was prepared from charred peanut shells as described in Appendix A. The second sample, used in runs five through seven, came from commercially available sampling tubes. These tubes were manufactured by SKC, Inc. and came from lot #105. All of the samples analyzed were outgassed

by flowing nitrogen through them while being heated at 150 to 200°C for approximately ninety minutes. On run number four, the same material that was used in runs one through three, was outgassed over night, approximately 10 hours. When analyzed, the resulting surface areas deviation from the mean area[d] was within the standard deviation[e] and it was concluded that a ninety minute degassing would be sufficient for the remaining runs.

In order to obtain an evaluation of the activation process, two samples of charred peanut shells, runs eight and nine, which had not been activated, were analyzed for surface area. As shown in Table 3, the activation process significantly increased the surface area.

Due to the size of the equipment used in activating the charred peanut shells and the quantity of adsorbent required throughout the work, it was necessary to make many small batches of adsorbent. Each of the batches was made under the same conditions, but it was felt that by determining the specific surface area of a sample from each batch, a check could be instituted to record any variations. The standard deviation between the different batches was a little over

---

a. See reference 5.

b. Instruction manual, High Speed Surface Area Analyzer Model 2200, Micrometrics Instrument Corporation.

c. See reference 24.

d. Calculated from $\frac{1}{n} \sum_{i=1}^{n} x_i = \bar{x}$.

e. Calculated from $[\varepsilon x^2 - \frac{(\varepsilon x^2)}{n}]/n-1 = s_x$.

Table 3. Surface Area Analysis

Test	Weight (gm)	Surface Area Reading (m^2)	Specific Surface Area (m^2/gm)	Mean[d] m^2/gm	σ[e]
1[a]	0.3389	140.7	415.2		
2[b]	0.3031	126.6	417.7		
3[b]	0.3598	140.5	390.5	397.9	17.3
4[b]	0.3634	140.1	385.5		
5[c]	0.9661	27.5	28.5	27.7	1.1
6[c]	0.2043	5.5	26.9		
7[d]	0.2700	76.8	284.5		
8[d]	0.2397	76.9	320.8		
9[d]	0.2784	98.1	352.4	336.8	38.0
10[d]	0.1323	46.5	351.5		
11[d]	0.2928	92.7	316.6		
12[d]	0.2303	90.9	394.7		
13[e]	0.1016	101.8	1002.0		
14[e]	0.0675	66.9	991.1	1006.2	17.6
15[e]	0.1228	125.9	1025.6		

a. Charred and activated peanut shell, out gassed at 175 degrees C for ten hours.

b. Same sample as a, out gassed at 175 degrees C for ninety minutes.

c. Charred peanut shell, not activated but outgassed ninety minutes.

d. Charred and activated peanut shells from six different batches, all outgassed at 175 degrees for ninety minutes.

e. Charcoal from SKC, Inc. sampling tubes, lot #105 P. O. Box 8538, Pittsburgh, Pa. Outgassed for ninety minutes at 175 degrees C.

twice the standard error found in the analyzer. To smooth out the variations in the different batches, all of the samples were combined and thoroughly mixed.

B-2. Pore Volume Distribution

To determine the size range of the pores in the activated charcoal, a Mercury Penetration Porosimeter was used. The instrument indicates the quantity of mercury that may be forced under various pressures into the pores of the charcoal and into the void spaces among the particles. The charcoal was first dried in an oven for four days at 110 degrees C, then put under a vacuum to remove any vapors or previously adsorbed gases.

Mercury has reported measurements of contact angles with different materials from 112 to 142 degrees.[a] Any liquid which exhibits this great of contact angle will resist wetting a solid or penetrating pores. Mercury's surface tension of 474 dynes per centimeter at 25 degrees C requires a high externally applied pressure to overcome this resistance. As the pressure is increased the quantity of liquid forced into the pores increases in proportion to the differential pore volume. Therefore, increasing the pressure of the mercury on a material having a given void space and pore-size distribution results in a unique pressure-volume curve. For a detailed discussion of the instrument and interpretation of data, the instruction manual of the machine should be

consulted.[b]

Examination of Figure 11 shows no pore distribution in the range examined--down to the machine's limit at 40 Å in diameter. Fornwalt and Hutchins[c] and others[d,e] have shown that many gas adsorbent carbons have sharp distribution of pore diameters around 16 to 35 Å. With this information in mind, a surface area analysis was carried out on the data. This yielded a surface area of approximately 125 m^2/gm, which was a little more than half of the area indicated by nitrogen adsorption methods. Generally it has been found that there is much closer agreement between the two different methods.[f,g] Dubinin[h] has shown that micropores contribute a substantial amount to the total surface area of porous carbons. By applying the surface area determined by the nitrogen adsorption, see Appendix B-1, to the results from the porosimeter, a sharp rise in the curve, Figure 11, at a pressure around 60,000 to 75,000 psia would yield pore diameters in the expected size range. Unfortunately, other methods such as small-angle x-ray scattering and a complete BET isotherm which have been shown to be fairly reliable in this pore size range,[c,d,e,i,j] were not available to confirm this hypothesis. It should also be noted that at high pressures, there is a possibility that the mercury may crush the pore structure. Scholten[k] has reviewed several investigations in this area. One charcoal was reported as being crushed by pressures above 500 atmospheres and another made of lignin

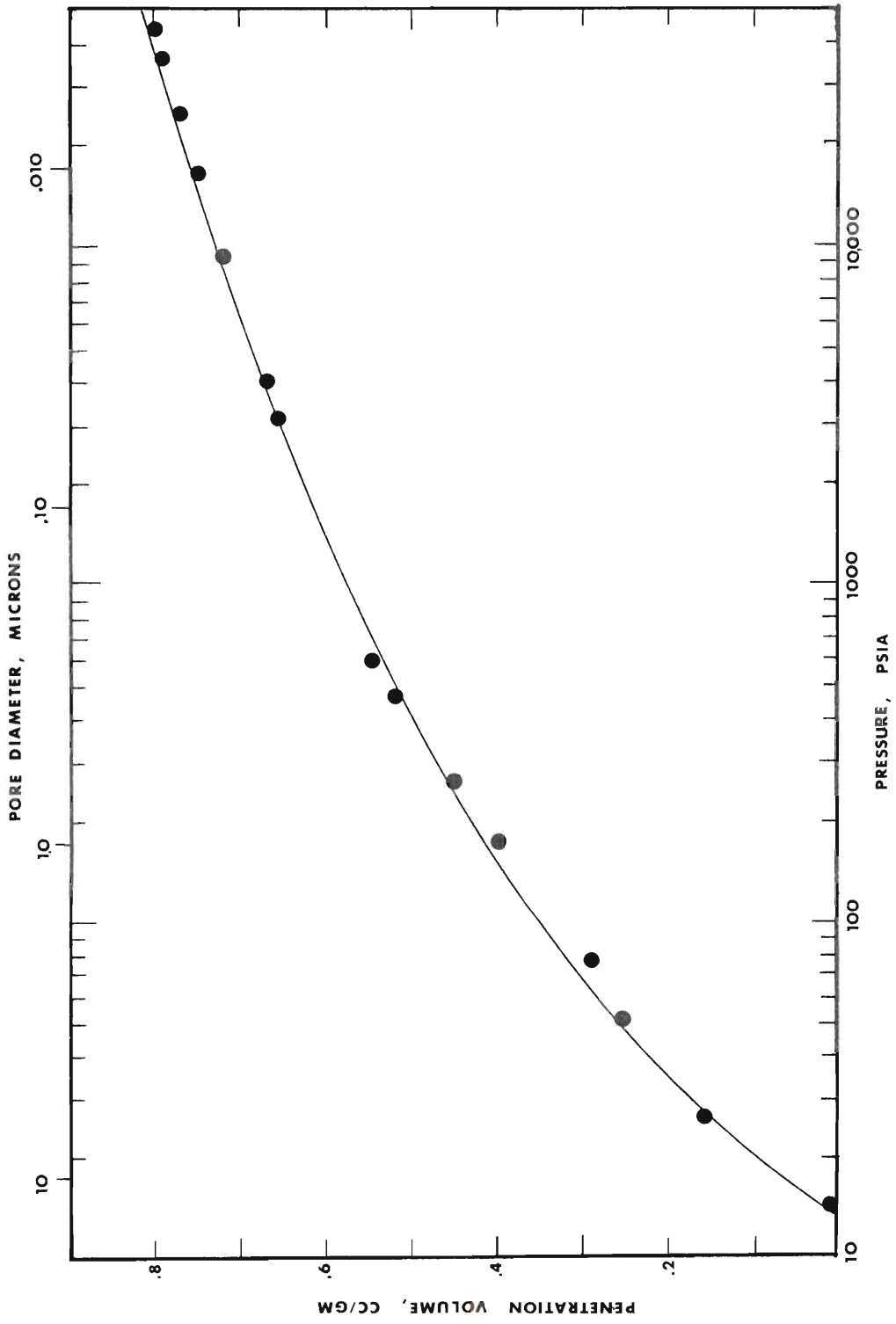

Figure 11. Penetration Volume - Pressure Curve from Mercury Porosimeter

went up to 2000 atmospheres with no crushing. Generally, the starting material was considered to be the determining factor in what pressure the charcoal would withstand.

B-3. Apparent and Particle Density

Apparent and particle density must be determined in order to calculate the void fraction in the bed, which is often used in evaluation of the adsorption characteristics of charcoals. The procedure used to determine the apparent or bulk density of the charcoal followed the ASTM standard method test D2854-70. An adequate sample of carbon to be tested was placed in an oven at 110 degrees C for three hours. A tared graduated cylinder was then filled at a uniform rate so that packing would also be uniform. The volume of

---

a. See reference 26.

b. Instruction Manual, Model 900/910 series Mercury Penetration Porosimeter, Micromeritics Instrument Corporation; Revised 4/20/70.

c. See reference 14.

d. See reference 11.

e. See reference 28.

f. See reference 16.

g. See reference 1.

h. See reference 10.

i. See reference 27.

j. See reference 12.

k. See reference 32.

charcoal in the graduated cylinder was then recorded to the nearest two tenths of a cubic centimeter (0.2 cc) and the weight of the sample to the nearest milligram. This test was performed on eight samples and yielded a mean bulk, or apparent, density of 0.216 grams per cubic centimeter, with a standard deviation of 0.004 grams per cubic centimeter.

Particle density, the weight under atmospheric pressure of a unit volume of carbon including pore volume but excluding inter-particle voids, was determined by mercury immersion. This was performed on a Micromeritics Instrument Corporation, Model 905-1, Mercury Penetration Porosimeter.[a] Sample density, ρ_s, at atmospheric pressure was calculated from the relationship:

$$\rho_s = \frac{W_s}{V - \left[\frac{(W_t - W_s - W_c)}{\rho} + (C_p + C_t)(\text{cell factor})\right]}$$

where V_c is the volume of the sample cell in cubic centimeters, ρ is the density of the mercury used, C_p is the corrected counter reading and C_t is a constant 2935. The cell factor used was 0.000781 cc/count. W_t is the total weight of sample cell, mercury, and sample after the penetration, W_s, the sample weight and W_c, the empty cell weight. Using this relationship, the particle density was determined to be 1.33 grams per cubic centimeter. Spencer[b] reports that

a. Instruction Manual, Model 900/910 series Mercury Penetration Porosimeter, Micromeritics Instrument Corporation; Revised 4/20/70.

b. See reference 34.

only a negligible amount of the porosity present is accessible to mercury under the applied pressure of one atmosphere used for density determination. This method was recommended for particle sizes greater than 100 mesh.

B-4. Total Ash Content of Activated Carbon

To characterize further the carbon used in this work, a total ash content test was carried out. Basically, this test followed ASTM standard method test D2866-70. A crucible was placed over a Bunsen burner and heated for approximately one hour. The crucible was then placed in a desiccator and allowed to cool to room temperature and weighed to the nearest 0.1 mg. An adequate sample of activated carbon was placed in an oven and dried for approximately 24 hours at 110 degrees centigrade. A portion of this dried sample was weighed to the nearest 0.1 mg in the crucible and then burned over a Bunsen burner for 15 hours. The crucible and ash were then placed in the desiccator and allowed to cool to room temperature. The crucible plus the ashed sample were reweighed to the nearest 0.1 mg. By dividing the weight of the ashed sample by the original sample weight, after subtracting the crucible weight, the total ash fraction is determined.

The test was carried out on three of the original seven batches of activated carbon. These tests showed 13.3, 15.1 and 13.3 percent ash content.

APPENDIX C

CALIBRATIONS

C-1. Calibration of Tube Flow Meters

Two Matheson Gas Products, Model 602, flow meters were used to monitor the flow of nitrogen and the nitrogen-sulfur dioxide mixture in this work. To obtain accurate results, a calibration chart was constructed for each flow meter. To do this, a wet test meter manufactured by Precision Scientific Company was used. The pressure and temperature of the gases were monitored and kept constant at one atmosphere and 25 degrees centigrade respectively. At each division on the flow meters, five different readings were made and then averaged together to provide a single point for the calibration chart. The average wet test meter reading points were then used in an nth order regression analysis program to generate a polynomial which best fits the data. See Figure 12 and Table 4. The data of Flow Meter 3 were best fitted with a fourth order polynomial.

$$Y(\text{Flow Rate}) = 11.6302 + .3097\ X + .4529 \times 10^{-1}\ X^2 + .1303 \times 10^{-3}\ X^3 - .1449 \times 10^{-5}\ X^4$$

The average deviation of the points generated by this

equation from the actual flow rates was 1.8 percent. The data of Flow Meter 5 were best fitted with a third order polynomial. See Figure 13 and Table 5.

$$Y \text{ (Flow Rate)} = 44.477 + .340\ X + .1137\ X^2 - .5589 \times 10^{-3}\ X^3$$

This equation gave an average deviation of 1.2 percent from the actual readings. These equations are plotted in Figures 12 and 13 and the average wet test meter readings are shown in each. Several measurements of different concentrations of sulfur dioxide and nitrogen showed insignificant variation from the runs with pure nitrogen.

C-2. Calibration of Infrared Analyzer

Gas flow compositions were monitored with a Beckman, Model 215A, Infrared Analyzer. A Sargent, Model MR, recorder was interfaced with the analyzer to provide a hard copy of the analysis for computational purposes. The analyzer determines the concentration of a particular component of interest by measuring the differential absorption of infrared energy between a reference energy beam and a sample energy beam. The analyzer consists of three electrically interconnected units: an analyzer section, an amplifier/control section, and a constant-voltage transformer.

The analyzer section contains a sample cell which is a flow-through tube that receives a continuous stream of

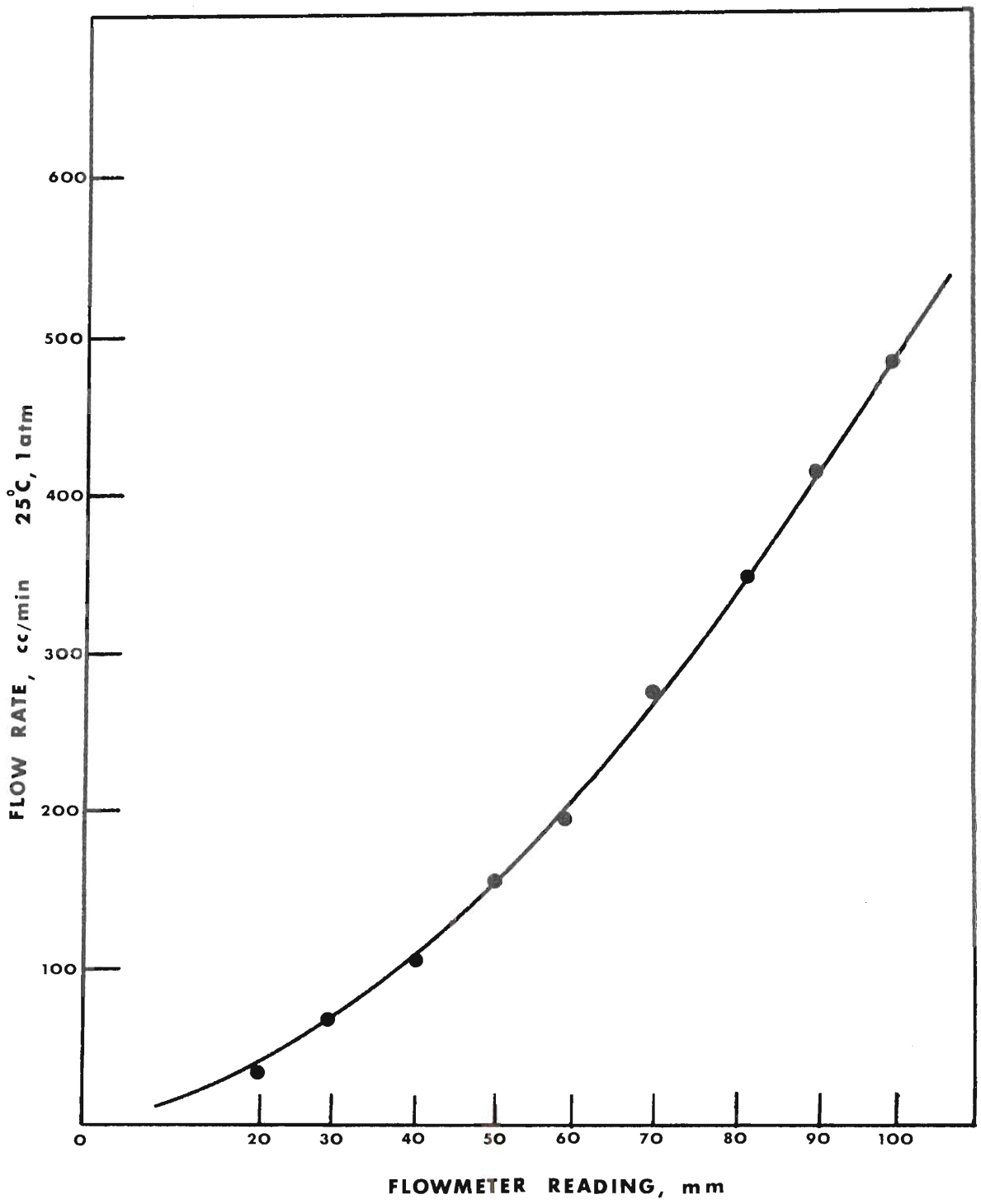

Figure 12. Calibration Curve for Flow Meter 3

Table 4. Calibration of Tube Flow Meter 3

Flow Meter Reading (mm)	Average Wet Test Meter Reading (cc/min)	Polynomial Fit Reading (cc/min)	Polynomial Deviation %
20	35	36	2.9
30	67	64	4.5
40	101	101	0
50	151	148	2.0
60	194	203	4.6
70	268	265	1.1
80	330	334	1.2
90	414	406	1.9
100	483	481	0.4
110	549	555	1.1
130	691	690	0.1

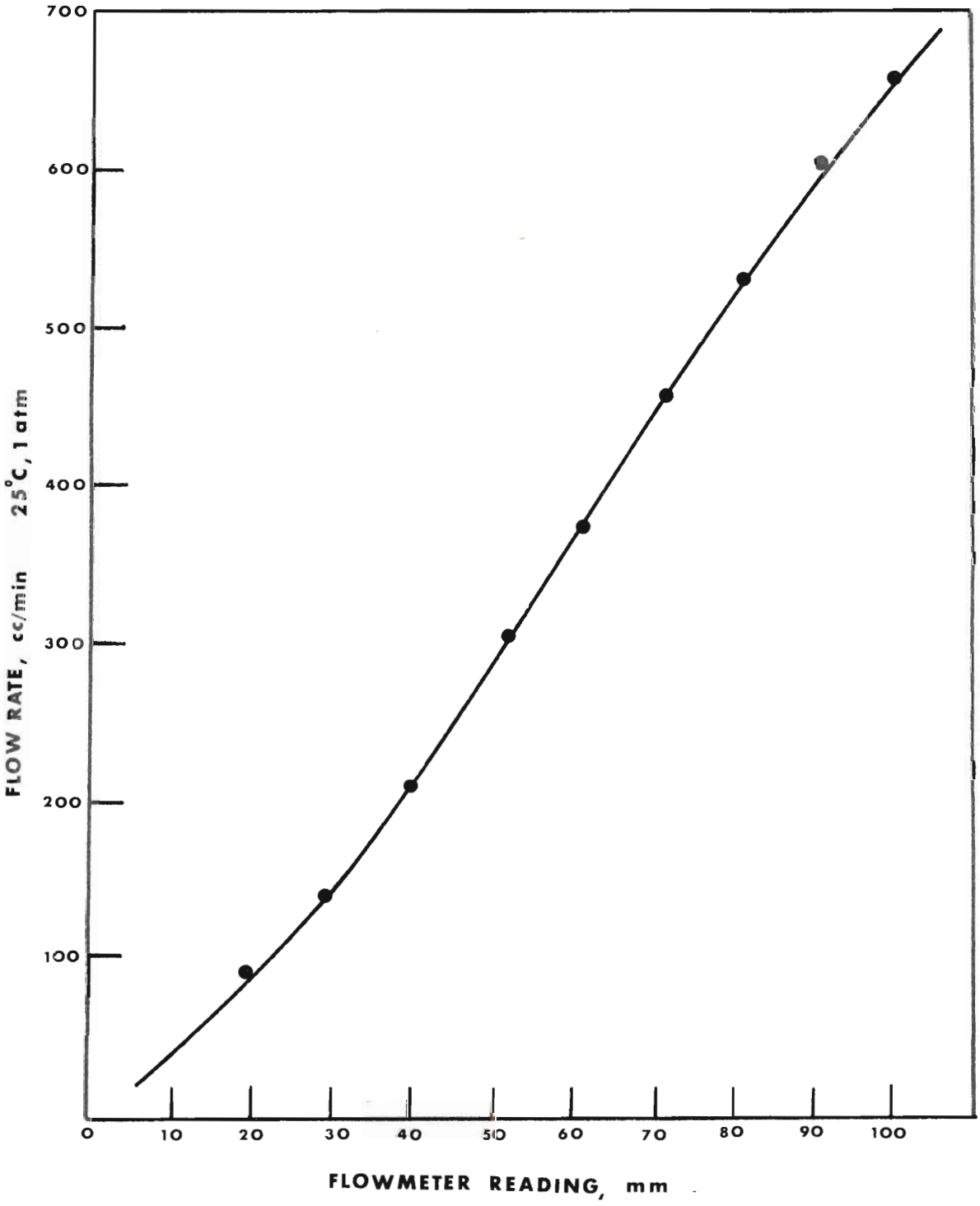

Figure 13. Calibration Curve for Flow Meter 5

Table 5. Calibration of Tube Flow Meter 5

Flow Meter Reading (mm)	Average Wet Test Meter Reading (cc/min)	Polynomial Fit Reading (cc/min)	Polynomial Deviation (%)
10	60	59	1.7
20	90	92	2.2
30	144	142	1.4
40	201	204	1.5
50	275	276	0.4
60	356	353	0.8
70	437	433	0.9
80	515	513	0.4
90	579	588	1.6
100	661	656	0.8

sample gas and a reference cell which is sealed and filled with a reference gas. Two energy beams which are directed through the cells are blocked simultaneously ten times per second by a two-segmented blade rotating at 5 revolutions per second. When the beam is not blocked, the presence of infrared-absorbing components in the sample stream cause a difference in energy levels when compared with the reference cell. This differential is detected by a sequence of transformations which take place in the two cells. In the sample cell, part of the original energy of the sample beam is absorbed by the sulfur dioxide flowing through. The reference cell is filled with nitrogen, which absorbs less energy. Each of the energy beams heats the gases in the cells. Due to the different absorption characteristics, the gas in the reference cell becomes hotter and thus the pressure within the cell becomes greater. As the pressure increases, a diaphragm at the end of the chamber flexes. The diaphragm and an adjacent stationary metal button constitute a two plate variable capacitor. In the amplier/control section, a ten Hertz output signal from the analyzer section is coupled to a gain control potentiometer. This control is used in calibrating the instrument for a different concentration of sample gas. The instruction manual should be consulted for a more detailed review.[a]

After allowing the infrared analyzer to warm to operating temperature, pure nitrogen was passed through it

and the scale was zeroed. The sulfur dioxide-nitrogen gas mixture used for the up-scale calibration was obtained from Matheson Gas Products, cylinder number 45563, and was analyzed and certified by the producer to be 5484 ppm by volume sulfur dioxide. One hundred percent of scale on the Infrared Analyzer therefore signified a 5484 ppm concentration of sulfur dioxide. A chart recorder, Sargent Model MR,[b] was then interfaced with the analyzer so that a recording of the analyzer's scale change, and thus a change in the sulfur dioxide concentration in the sample gas, could be recorded as a function of time. See Table 6. Due to the nonlinear response of the analyzer to changes in sample gas concentration, a concentration-instrument response calibration curve was plotted as seen in Figure 14. By varying the flow rates of the two streams of gases and recording the response on the analyzer scale, the various points for this graph were obtained. The actual flow rates were determined by the equations generated from the regression analysis program run on each flow meter. The data for the Infrared analyzer calibration was also fit to a polynomial expression for computational purposes. A fifth order equation

$$Y\ (\text{concentration}) = -22.176 + 44.117X - 2.186\ X^2 + 0.794 \times 10^{-1}\ X^3 - 0.106 \times 10^{-2}\ X^4 + 0.495 \times 10^{-5}\ X^5$$

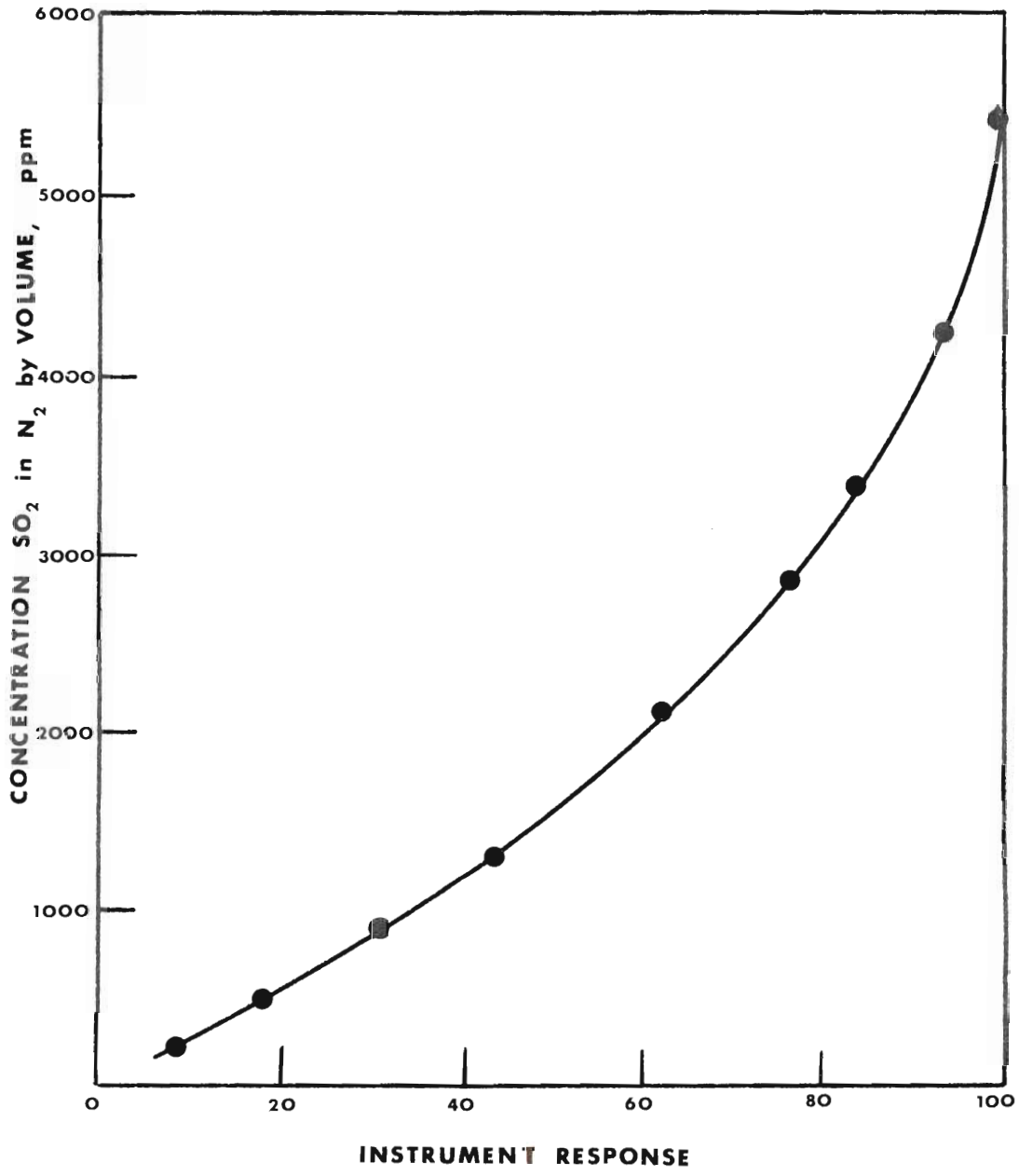

Figure 14. Concentration-Instrument Response Calibration Curve

Table 6. Concentration-Instrument Response Data

Test #	Flow Meter #3 Reading (mm)	Flow Rate (cc/min)	Flow Meter #5 Reading (mm)	Flow Rate (cc/min)	(#3/#5) 5484 (ppm SO_2)	Instrument Response
1	94	436	70	434	5509	100 0
2	85	369	70	434	4663	97.5
3	80	334	70	434	4220	94.0
4	75	290	70	434	3664	90.0
5	71	272	70	434	3437	85.0
6	61	209	70	434	2641	73.5
7	55	174	70	434	2199	64.7
8	50	148	70	434	1870	58.0
9	45	123	70	434	1554	50.7
10	40	101	70	434	1276	43.0
11	30	64	70	434	808	31.5
12	25	49	70	434	619	24.5
13	20	35	70	434	442	18.7
14	10	17	70	434	214	9.7
15	0	0	70	434	0	0.0

gave a mean deviation from actual results of 4.5 percent.

---

a. Instruction Manual, Beckman Models 215A, 315A, and 415A Infrared Analyzer Beckman Instruments, Inc.; Fullerton, California 92634

b. Instruction Manual, Sargent Recorder Model MR. E. H. Sargent and Company; Chicago, Illinois 60630.

APPENDIX D

EXPERIMENTAL DATA

Test 53, T = 25°C, F = 100 cc/min, C_o = 5484 ppm SO_2, Carbon 3.018 gm

Time (min)	Instrument Response	Concentration (ppm SO_2)	C/C_o
174.0	2.5	76	0.014
177.0	14.5	356	0.065
178.5	33.5	861	0.157
179.4	44.0	1294	0.236
180.9	58.0	1928	0.352
181.5	62.5	2127	0.388
184.5	75.0	2695	0.491
185.1	82.0	3102	0.566
186.0	87.0	3500	0.638

Test 55, T = 25°C, F = 175 cc/min, C_o = 5484 ppm SO_2, Carbon 3.055 gm

Time (min)	Instrument Response	Concentration (ppm SO_2)	C/C_o
72.0	3.5	108	0.020
80.1	10.0	270	0.049
81.9	24.5	576	0.105
82.5	35.0	918	0.167
83.1	45.0	1339	0.244
83.7	53.5	1725	0.315
85.5	70.0	2458	0.448
87.0	83.0	3172	0.579
88.5	92.0	4048	0.738
90.6	94.0	4327	0.789

Test 56, T = 25°C, F = 250 cc/min, C_o = 5484 ppm SO_2, Carbon 3.049 gm

Time (min)	Instrument Response	Concentration (ppm SO_2)	C/C_o
64.2	2.0	58	0.011
66.0	27.5	661	0.120
66.9	45.0	1339	0.244
67.8	57.5	1906	0.348
68.4	64.0	2193	0.400
69.0	69.0	2413	0.440
70.5	81.5	3068	0.560
71.1	85.0	3326	0.607

Test 4, T = 25°C, F = 350 cc/min, C_o = 5484 ppm SO_2, Carbon 3.003 gm

Time (min)	Instrument Response	Concentration (ppm SO_2)	C/C_o
30.6	2.0	58	0.011
31.2	13.0	328	0.060
32.4	38.0	1037	0.189
33.6	56.5	1861	0.339
34.8	67.0	2324	0.424
35.9	76.0	2746	0.501
38.0	86.5	3455	0.630
38.4	89.5	3752	0.684
40.8	95.0	4480	0.817

Test 57, T = 25°C, F = 500 cc/min, C_o = 5484 ppm SO_2, Carbon 3.000 gm

Time (min)	Instrument Response	Concentration (ppm SO_2)	C/C_o
27.8	6.5	192	0.035
28.2	18.5	435	0.079
28.6	38.5	1057	0.193
28.8	49.0	1520	0.277
29.6	72.0	2550	0.465
30.0	76.5	2772	0.506
30.2	84.0	3247	0.599
30.4	89.5	3751	0.684
31.1	92.0	4049	0.738

Test 54, T = 25°C, F = 700 cc/min, C_o = 5484 ppm SO_2, Carbon 3.015 gm

Time (min)	Instrument Response	Concentration (ppm SO_2)	C/C_o
16.4	4.5	139	0.025
16.8	19.0	446	0.081
17.2	40.0	1120	0.204
17.6	57.5	1906	0.348
18.0	70.0	2458	0.448
19.6	85.0	3326	0.607
19.8	95.0	4480	0.817
19.9	96.2	4679	0.853
20.0	97.5	4915	0.896

Test 29, T = 50°C, F = 100 cc/min, C_o = 5484 ppm SO_2, Carbon 3.032 gm

Time (min)	Instrument Response	Concentration (ppm SO_2)	C/C_o
130.0	5.0	153	0.028
132.0	9.5	259	0.047
132.9	20.0	467	0.085
134.2	34.0	879	0.160
136.0	51.5	1634	0.298
137.8	65.5	2258	0.412
140.2	76.0	2746	0.501
141.0	85.0	3326	0.607

Test 9, T = 50°C, F = 175 cc/min, C_o = 5484 ppm SO_2, Carbon 2.989 gm

Time (min)	Instrument Response	Concentration (ppm SO_2)	C/C_o
66.3	4.0	124	0.023
67.5	20.5	478	0.087
68.1	42.0	1205	0.220
69.0	60.0	2017	0.368
69.6	68.2	2377	0.433
70.8	76.5	2772	0.506
73.5	85.0	3326	0.607
78.0	92.5	4115	0.750
81.0	95.5	4561	0.832

Test 19, T = 50°C, F = 250 cc/min, C_o = 5484 ppm SO_2, Carbon 3.115 gm

Time (min)	Instrument Response	Concentration (ppm SO_2)	C/C_o
36.0	3.5	109	0.020
41.4	23.5	550	0.100
42.0	44.5	1316	0.240
43.0	70.0	2458	0.448
44.4	85.0	3326	0.607
45.0	90.5	3865	0.705
46.8	97.0	4822	0.879
49.2	99.0	5213	0.951

Test 20, T = 50°C, F = 350 cc/min, C_o = 5484 ppm SO_2, Carbon 2.937 gm

Time (min)	Instrument Response	Concentration (ppm SO_2)	C/C_o
23.4	3.0	93	0.017
24.6	26.0	617	0.113
25.8	47.0	1428	0.261
27.0	61.5	2083	0.380
27.6	67.5	2346	0.428
28.8	75.0	2695	0.491
29.4	79.0	2912	0.531
30.0	82.5	3137	0.572
30.6	85.5	3367	0.614
34.5	91.0	3924	0.716

Test 10, T = 50°C, F = 500 cc/min, C_o = 5484 ppm SO_2, Carbon 3.053 gm

Time (min)	Instrument Response	Concentration (ppm SO_2)	C/C_o
18.9	5.2	159	0.029
19.5	17.5	415	0.076
20.1	41.5	1184	0.216
20.7	63.5	2171	0.396
21.0	72.0	2549	0.465
22.5	89.8	3785	0.690
23.1	91.6	3998	0.729
24.0	93.3	4225	0.770

Test 8, T = 50°C, F = 700 cc/min, C_o = 5484 ppm SO_2, Carbon 3.010 gm

Time (min)	Instrument Response	Concentration (ppm SO_2)	C/C_o
12 0	2.5	76	0.014
12.6	25.0	589	0.107
12.9	42.0	1206	0.220
13.2	53.5	1725	0.315
13.5	62.5	2127	0.388
13.8	70.0	2458	0.448
14.4	80.5	3003	0.548
15.0	87.0	3499	0.638
15.9	92.5	4115	0.750
16.8	95.0	4480	0.817

Test 17, T = 75°C, F = 100 cc/min, C_o = 5484 ppm SO_2, Carbon 3.100 gm

Time (min)	Instrument Response	Concentration (ppm SO_2)	C/C_o
85.5	2.5	76	0.014
87.0	23.0	537	0.098
87.9	44.0	1294	0.236
88.2	51.0	1611	0.294
89.1	66.0	2280	0.416
89.4	69.0	2413	0.440
90.6	77.5	2826	0.515
91.8	82.5	3137	0.572
92.4	84.0	3247	0.592

Test 15, T = 75°C, F = 175 cc/min, C_o = 5484 ppm SO_2, Carbon 3.093 gm

Time (min)	Instrument Response	Concentration (ppm SO_2)	C/C_o
48.6	3.0	93	0.017
49.8	25.5	603	0.110
50.1	37.0	996	0.182
50.7	55.5	1816	0.331
51.6	73 0	2597	0.474
52.8	85.2	3343	0.610
54.0	90 .5	3865	0.705
55.8	94.0	4327	0.789
57.0	95.5	4561	0.832

Test 31, T = 75°C, F = 250 cc/min, C_o = 5484 ppm SO_2, Carbon 3.027 gm

Time (min)	Instrument Response	Concentration (ppm SO_2)	C/C_o
30.2	5.0	153	0.028
30.6	10.5	280	0.051
31.2	33 0	843	0.154
31.5	43.5	1271	0.232
31.8	51.5	1634	0.298
32.1	58 0	1928	0.352
32.4	65.0	2236	0.408
33.0	74.5	2669	0.487
33.6	80.1	2972	0.542

Test 13, T = 75°C, F = 350 cc/min, C_o = 5484 ppm SO_2, Carbon 3.109 gm

Time (min)	Instrument Response	Concentration (ppm SO_2)	C/C_o
19 8	4.5	139	0.025
20.7	26.5	631	0.115
21.0	36.0	956	0.174
21.9	53.0	1703	0.310
22.8	64.0	2193	0.400
24.0	75.0	2695	0.491
25.8	85.0	3326	0.607
27.6	90.7	3889	0.709
28.8	93.0	4183	0.763

Test 18, T = 75°C, F = 500 cc/min, C_o = 5484 ppm SO_2, Carbon 2.957 gm

Time (min)	Instrument Response	Concentration (ppm SO_2)	C/C_o
11.4	4.0	124	0.023
12.0	17.0	405	0.074
12.6	39 0	1078	0.197
12.9	47.5	1452	0.265
13.2	55.0	1793	0.327
13.8	69.5	2435	0.444
14.7	82.5	3137	0.572
15.0	85.0	3326	0.607
15.9	90.5	3865	0.705
16.4	92.0	4049	0.738

Test 14, T = 75°C, F = 700 cc/min, C_o = 5484 ppm SO_2, Carbon 3.029 gm

Time (min)	Instrument Response	Concentration (ppm SO_2)	C/C_o
8.9	4.0	124	0.023
9.5	22.5	525	0.096
9.8	45.0	1339	0.244
10.1	61.0	2061	0.376
10.2	65.0	2237	0.408
10.6	76.5	2772	0.506
11.0	82.5	3137	0.572
11.9	90.0	3807	0.694
12.5	93.0	4183	0.763

Test 28, T = 100°C, F = 100 cc/min, C_o = 5484 ppm SO_2, Carbon 3.024 gm

Time (min)	Instrument Response	Concentration (ppm SO_2)	C/C_o
63.6	2.0	58	0.011
64.8	22.5	525	0.096
65.4	36.0	956	0.174
66.0	47.0	1429	0.261
66.6	57.0	1883	0.343
67.2	64.5	2215	0.404
68.4	75.5	2720	0.496
69.0	78.5	2883	0.526
70.0	81.0	3035	0.554

Test 27, T = 100°C, F = 175 cc/min, C_o = 5484 ppm SO_2, Carbon 3.009 gm

Time (min)	Instrument Response	Concentration (ppm SO_2)	C/C_o
38.1	4 0	125	0.023
38.7	27.0	646	0.118
39.0	41.5	1148	0.216
39.3	53.0	1703	0.310
39.6	62.5	2127	0.388
40.2	74.0	2645	0.482
40.5	79.0	2912	0.531
41.1	85.5	3368	0.614
42.0	90.0	3807	0.694

Test 30, T = 100°C, F = 250 cc/min, C_o = 5484 ppm SO_2, Carbon 2.976 gm

Time (min)	Instrument Response	Concentration (ppm SO_2)	C/C_o
22.5	4.5	139	0.025
23.1	24.0	563	0.103
23.4	35.0	918	0.167
24.0	52.5	1679	0.306
24.6	65.5	2258	0.412
25.8	81.5	3068	0.560
28.2	89.5	3751	0.684
30.0	94.0	4326	0.789
31.8	98.0	5010	0.914
33.0	99.5	5319	0.970

Test 23, T = 100°C, F = 350 cc/min, C_o = 5484 ppm SO_2, Carbon 3.103 gm

Time (min)	Instrument Response	Concentration (ppm SO_2)	C/C_o
14.1	5.0	153	0.028
14.7	25.0	589	0.107
15.0	40.5	1141	0.208
15.3	55.0	1793	0.327
15.6	65.0	2237	0.408
15.9	75.0	2695	0.491
16.2	82.0	3102	0.566
16.5	85.0	3326	0.607
16.8	88.0	3596	0.656
17.4	90.5	3866	0.705

Test 26 , T = 100°C, F = 500 cc/min, C_o = 5484 ppm SO_2, Carbon 3.084 gm

Time (min)	Instrument Response	Concentration (ppm SO_2)	C/C_o
9.6	4.5	139	0.025
9.8	23.5	550	0.100
9.9	36.0	956	0.174
10 0	47.5	1452	0.265
10.2	61.5	2083	0.380
10.3	66.5	2303	0.420
10.5	74.0	2645	0.482
11.0	84.0	3247	0.592
11.4	87.5	3547	0.647
12.0	90.0	3807	0.694

Test 25, T = 100°C, F = 700 cc/min, C_o = 5484 ppm SO_2, Carbon 3.119 gm

Time (min)	Instrument Response	Concentration (ppm SO_2)	C/C_o
7.0	10.0	270	0.049
7.1	20 0	467	0.085
7.2	32.0	808	0.147
7.3	43.3	1263	0.230
7.5	61.0	2061	0.376
7.6	68.0	2368	0.432
7.8	77.0	2799	0.510
8.2	85.5	3368	0.614
8.4	87.5	3547	0.647
9.0	90.5	3865	0.705
11.0	94.5	4402	0.803

Test 34, T = 125°C, F = 100 cc/min, C_o = 5484 ppm SO_2, Carbon 3.055 gm

Time (min)	Instrument Response	Concentration (ppm SO_2)	C/C_o
48.0	6.5	192	0.035
48.6	22.0	513	0.094
48.9	32.0	808	0.147
49.5	49.0	1520	0.277
49.8	55.5	1816	0.331
50.1	60.5	2039	0.372
50.4	65.0	2236	0.408
51.6	76 0	2746	0.501
52.2	81.5	3068	0.560
52.8	87.0	3499	0.638

Test 35, T = 125°C, F = 175 cc/min, C_o = 5484 ppm SO_2, Carbon 2.940 gm

Time (min)	Instrument Response	Concentration (ppm SO_2)	C/C_o
28.2	7.5	216	0.039
28.8	22.5	525	0.096
29.1	31.0	773	0.141
29.4	39.0	1078	0.197
29.7	48.0	1474	0.269
30.0	57.0	1884	0.343
31.2	79.5	2942	0.536
31.8	85.0	3326	0.607
33.0	95.0	4480	0.817

Test 36, T = 125°C, F = 250 cc/min, C_o = 5484 ppm SO_2, Carbon 3.110 gm

Time (min)	Instrument Response	Concentration (ppm SO_2)	C/C_o
18.3	11.5	299	0.055
18.6	29.5	723	0.132
18.9	44 5	1316	0.240
19.2	55.0	1793	0.327
19.5	64.5	2215	0.404
19.8	71.0	2503	0.456
20.1	77.5	2826	0.515
21.0	86.5	3455	0.630
21.6	89.5	3751	0.684
22.8	92.5	4115	0.750

Test 33 , T = 125°C, F = 350 cc/min, C_o = 5484 ppm SO_2, Carbon 2.998 gm

Time (min)	Instrument Response	Concentration (ppm SO_2)	C/C_o
10.8	13.0	327	0.060
11.0	30.0	739	0.135
11.2	46.5	1406	0.256
11.4	60.0	2017	0.368
11.6	70.0	2458	0.448
11.8	77.0	2799	0.510
12.4	87.0	3499	0.638
13.6	91.0	3924	0.716
14.0	94.5	4402	0.803

Test 40, T = 125°C, F = 500 cc/min, C_o = 5484 ppm SO_2, Carbon 2.990 gm

Time (min)	Instrument Response	Concentration (ppm SO_2)	C/C_o
7.9	5.0	153	0.028
8.2	19.5	456	0.083
8.4	32.0	808	0.147
8.6	44.0	1294	0.236
8.8	55.5	1816	0.331
9.0	65.0	2237	0.408
9.2	72.0	2550	0.465
9.6	81.0	3035	0.554
10.0	86.5	3455	0.630
10.8	92.5	4115	0.750

Test 39, T = 125°C, F = 700 cc/min, C_o = 5484 ppm SO_2, Carbon 3.044 gm

Time (min)	Instrument Response	Concentration (ppm SO_2)	C/C_o
6.0	3.5	108	0 020
6.1	15.0	366	0.067
6.3	41.0	1163	0.212
6.4	50.5	1588	0.290
6.5	57.5	1906	0.348
6.7	69.0	2413	0.440
7.0	81.5	3068	0.560
7.2	86.0	3410	0.622
7.8	93.0	4183	0.763
8.5	95.0	4480	0.817

BIBLIOGRAPHY

1. Adamson, Arthur W., Physical Chemistry of Surfaces, 2nd Ed. Interscience Publishers, New York (1967).

2. Allen, J. B., Joyce, R. S., and Kasch, R. H., "Process Design Calculations for Adsorption from Liquids in Fixed Beds of Granular Activated Carbon," Journal of the Water Pollution Federation 39 (2) 217 (1967).

3. Barnebey, H. L. in Lee, N. Y. and Zwiebel, Imre, Ed., "Activated Charcoal in the Petrochemical Industry," Adsorption Technology, 67 (117) American Institute of Chemical Engineers, New York (1971).

4. Brocke, Werner, "Prospects for the Practical Application of Flue Gas Desulfurization," Staub-Reinhalt Luft 28 (3), 112 (1968).

5. Brunauer, S., Emmett, P. H., and Teller, E., "The Adsorption of Gases in Multimolecular Layers," Journal of the American Chemical Society 60, 309 (1938).

6. Courouleau, P. H., and Benson, R. E., "Activated Carbon, Manufacture, Capacity of Adsorption, Use in Solvent Recovery," Chemical Engineering 55 (3), 112 (1948).

7. Dacey, J. R., in Flood, E. A.; Ed., "Active Carbon," The Solid-Gas Interface, Vol. 2, Marcel Dekker, Inc., New York (1967).

8. Deitz, Victor R., Bibliography of Solid Adsorbents, United States Cane Sugar Refiners and Bone Char Manufactures and National Bureau of Standards, Washington, D. C. (1944).

9. Dratwa, Heinrich and Juntgen, Harald, "The Desulfurization of Flue Gas by Means of Adsorption Cokes with Various Properties," Staub-Reinhalt Luft 27 (7) 1 (1967).

10. Dubinin, M. M., "Porous Structure and Adsorption Properties of Active Carbons," Carbon 2, 51 (1964).

11. Dubinin, M. M., Plavnik, G. M., and Zaverina, E. D., "Integrated Study of the Porous Structure of Active Carbons from Carbonized Sucrose," Carbon 2, 261 (1964).

12. Eanes, E. D., and Posner, A. S., in Flood, E. A.; Ed., "Small Angle X-Ray Scattering Measurements of Surface Areas," The Solid-Gas Interface, Vol. 2, Marcel Dekker, Inc., New York (1967).

13. Engel, H. C., and Coull, James, "Adsorption Studies of Vapors in Carbon Packed Towers," Transactions of the American Institute of Chemical Engineers 38 947 (1942).

14. Fornwalt, H. J., and Hutchins, R. A., "Purifying Liquids with Activated Carbon," Chemical Engineering 73 April 11 (1966).

15. Hatfield, A., "The Adsorption of Sulfur Dioxide on Activated Carbons from Peanut Hulls and Waste Rubber," M.S. Thesis, Georgia Institute of Technology (1976).

16. Joyner, L. G., Barret, E. P., and Skold, R., "Determination of Pore Volume and Area Distributions in Porous Substances; Comparison Between Nitrogen Isotherm and Mercury Porosimeter Methods," J. Am. Chem. Soc. 73, 1355 (1951).

17. Juntgen, H., and Peters, W., "Results of Recent Research in Waste Gas," Staub-Reinhalt Luft 28 (3) 89 (1968).

18. Juntgen, H., and Peters, W., "Technical Principles of Separating SO_2 from Waste Gases," Staub-Reinhalt Luft 25 (10) 60 (1965).

19. Kidney, Arthur J., "The Kinetics of Adsorption of Methane and Nitrogen from Hydrogen Gas," Ph.D. Dissertation, Colorado School of Mines (1968).

20. Lee, Hanju, and Stahl, D. E., "Oxygen Rich Gas from Air by Pressure Swing Adsorption Process," in AICHE Symposium Series Gas Purification by Adsorption, 69, (134) 1355 American Institute of Chemical Engineers (1973).

21. Linsen, B. D., and Heuvel, A. Van der, in Flood, E. A.; Ed. "Pore Structures," The Solid-Gas Interface, Vol. 2, Marcel Dekker, Inc., New York (1967).

22. Mantell, C. L., Industrial Carbon, Its Elemental, Adsorptive, and Manufactured Forms, 2nd Ed., D. Van Nostrand Company, Inc., New York (1946).

23. Mattson, James S., and Mark, Harry B., Activated Carbon, Marcel Dekker, Inc., New York (1971).

24. McCellan, Al, and Harnsberger, H. F., "Cross Sectional Areas of Molecules Adsorbed on Solid Surfaces," Journal of Colloid and Interface Science 23, 577 (1967).

25. Mahajan, O. P., Morishita, M., and Walker, P. L., Jr., "Dynamic Adsorption of Carbon Dioxide on Microporous Carbons," Carbon 8, 167 (1970).

26. Orr, C., Jr., and DallaValle, J. M., Fine Particle Measurement, The MacMillan Co., New York, N. Y. (1959).

27. Ponce, Vladimir, Knor, Zlatko, and Cerny, Slavoj, in English edited by Smith, D. ,and Adams, N. G., Adsorption on Solids, Butterworths Group, London and Publishers of Technical Literature, Prague (1974).

28. Rao, T. L. Narasimha, and Dater, D. S., "Active Carbon from Coconut Shell: Part I--Vapor Adsorbent Carbon," Indian Journal of Technology 2, 399 (1964).

29. Ray, G. C., and Box, E. O., Jr., "Adsorption of Gases on Activated Charcoal," Industrial and Engineering Chemistry 42, (7) 1315 (1949).

30. Rosen, J. B., "Kinetics of a Fixed Bed System for Solid Diffusion into Spherical Particles," The Journal of Chemical Physics 20 (3) 387 (1952).

31. Rosen, J. B., "General Numerical Solution for Solid Diffusion in Fixed Beds," Industrial and Engineering Chemistry, Engineering, Design, and Process Development 46 (8) 1590 (1954).

32. Scholten, J. J. F., in Bond, R. L.; Ed., "Mercury Porosimetry and Allied Techniques," Porous Carbon Solids, Academic Press, New York (1967).

33. Smith, J. M., Chemical Engineering Kinetics, 2nd Edition, McGraw-Hill, New York (1970).

34. Spencer, D. H. T., in Bond, R. L.; Ed., "The Use of Molecular Probes in the Characterization of Carbonaceous Material," Porous Carbon Solids, Academic Press, New York (1967).

35. Squires, Arthur M., "Air Pollution: The Control of SO_2 from Power Stacks: Part I, The Removal of Sulfur from Fuels," Chemical Engineering 74 (23) 260 (1967).

36. Squires, Arthur M., "Air Pollution: The Control of SO_2 from Power Stacks: Part II, The Removal of SO_2 from Stack Gases," Chemical Engineering 74, (24) 133 (1967).

37. Stacy, W. O., Vastola, F. J., and Walker, P. L., Jr., "Interaction of Sulfur Dioxide with Active Carbon," Carbon 6 917 (1968).

38. Strauss, Werner, in Strauss, Werner, Ed., Air Pollution Control Part I, Wiley-Interscience, New York (1971).

39. Thomas, J. M., and Thomas W. J., Introduction to the Principles of Heterogeneous Catalysis, Academic Press, London (1967).

40. Treybal, R. E., Mass Transfer Operations, 2nd Ed., McGraw-Hill, New York (1968).

41. Whitehead, T. H., and Sherrill, R. W., "Wood Charcoal from a Cinder Block Kiln," Forest Products Journal 11 (8) 336 (1961).

42. Zentgraf, K. M., "Full-Space Industrial Tests of Waste Gas Desulfurization," Staub-Reinhalt Luft 28 (3) 1 (1968).